# STRUCTURAL HEALTH MONITORING OF A TALL BUILDING

by
Erdinç Kırkpınar
B.S., Civil Engineering, Bogazici University, 2010

Submitted to the Institute for Graduate Studies in
Science and Engineering in partial fulfillment of
the requirements for the degree of
Master of Science

Graduate Program in Civil Engineering
Boğaziçi University
2013

STRUCTURAL HEALTH MONITORING OF A TALL BUILDING

APPROVED BY:

| | |
|---|---|
| Assist. Prof. Serdar Soyöz<br>(Thesis Advisor) | . . . . . |
| Assoc. Prof. Hilmi Luş | . . . . . |
| Assist. Prof. Ufuk Yazgan | . . . . . |

DATE OF APPROVAL: 12.06.2013

# ACKNOWLEDGEMENTS

I would like to express my gratitude to my supervisor, Assist. Prof. Serdar Soyöz for the guidance and support throughout my studies. His efforts and guidance led me in the pursuit of this master thesis and my future academic life. I would like to express my thanks to Assoc. Prof. Hilmi Luş for the advices and support as my academic advisor in my undergraduate years and for valuable contributions to my master thesis and to Assist. Prof. Ufuk Yazgan for his time and valuable suggestions.

I am also grateful to Prof. Engin Karaesmen and Prof. Erhan Karaesmen for their support in my Ph.D. application process. They are two of the most inspiring academicians in my life.

I am thankful to Mr. Faruk Duman for his help in every problem that I encountered during my field studies. Besides, I would like to thank Ms. Eda Gültekin for her help and guidance throughout my thesis year.

I would like to express my sincere gratitude to my beloved friends, Ms. Irmak Ertör and Ms. Pınar Ertör for their support and joy of living. I also want to thank my colleague, Mr. Ekin Özer, who helped me in my studies when I needed most.

I also would like to thank to people in DirenGezi!, showing the greatest struggle I am witnessed. They reminded me the feeling of hope again.

I am very thankful to my brothers, Mr. Kayahan Kaya, Mr. Meftun Çulpan and Mr. Serdarhan Aksoy. They make me feel I never walk alone.

Finally, I would like to show my greatest appreciation to my father Kenan Kırkpınar and to my mother Öznur Kırkpınar for their understanding, love and support throughout my life.

# ABSTRACT

## STRUCTURAL HEALTH MONITORING OF A TALL BUILDING

In mega cities such as Istanbul, tall buildings are inevitable outcomes of limited construction areas; however in earthquake prone mega cities again such as Istanbul, adequate precautionary measures for tall buildings must be taken before and after an expected earthquake. Structural health monitoring techniques have been used to understand existing conditions of structures, as well as their post-earthquake conditions. In order to investigate possible solutions to such necessities, a twenty-six story, core-wall tall building in Istanbul is instrumented with sixteen accelerometers. Natural frequencies and modal shapes of the building are obtained by frequency domain decomposition method. These results are compared with the modal values obtained from the finite element model of the building created according to design drawings. A finite element model updating process is applied. Time history analyses under probable earthquake input motions are performed. Analyses results are compared based on probability density functions. In this study it is shown that model updating based on identified modal values are significant in the determination of seismic demands on tall buildings.

# ÖZET

## YÜKSEK BİR BİNANIN YAPISAL SAĞLIK İZLEMESİ

İstanbul gibi mega şehirlerde yüksek binalar inşaat alanlarındaki yetersizliğin kaçınılmaz sonucudur. Ancak yine İstanbul gibi büyük deprem riski taşıyan kentlerde, olası bir depreme karşı öncesiyle ve sonrasıyla tüm önlemleri alınması gerekmektedir. Yapı sağlığı izleme teknikleri var olan binaların güvenlilik seviyelerini ve olası bir deprem sırasındaki performanslarını tespit edebilmek amacıyla kullanılmaktadır. Bu gibi ihtiyaçlara karşılık bulabilmek amacıyla, İstanbul sınırları içinde bulunan, 26 katlı, çekirdek perde duvar sistemi ile inşaa edilmiş bir yüksek bina 16 ivmeölçer ile izlenmektedir. Bu yapının doğal salınım frekansları ve mod şekilleri sistem tanılama yöntemi ile elde edilmiştir. Elde edilen sonuçlar mimari çizimlere gore hazırlanan sonlu elemanlar modelinden elde edilen sonuçlar ile karşılaştırılmıştır. Bunu takiben bir sonlu elemanlar model güncellemesi uygulanmıştır. Olası deprem kayıtları altında zaman tanım analizleri yapılmıştır. Analiz sonuçları olasılık yoğunluğu fonksiyonları temel alınarak karşılaştırımıştır. Bu çalışmayla gösterilmiştir ki, tanılanmış mod değerleri temel alınarak uygulanan sonlu elemanlar model güncellemesi, bina üzerine gelecek olan deprem yükü talebinin belirlenmesinde belirgin bir rol oynamaktadır.

# TABLE OF CONTENTS

ACKNOWLEDGEMENTS . . . . . iii
ABSTRACT . . . . . iv
ÖZET . . . . . v
LIST OF FIGURES . . . . . viii
LIST OF TABLES . . . . . xii
LIST OF SYMBOLS . . . . . xiii
LIST OF ACRONYMS / ABBREVIATIONS . . . . . xiii
1. INTRODUCTION . . . . . 1
1.1. Overview . . . . . 1
1.2. Literature Review . . . . . 2
1.3. Objective . . . . . 9
1.4. Scope of Study . . . . . 10
2. SYSTEM IDENTIFICATION . . . . . 12
2.1. General . . . . . 12
2.2. Digital Signal Processing . . . . . 13
2.2.1. Signals in Time Domain . . . . . 13
2.2.2. Cross Power Spectral Density . . . . . 14
2.2.3. Problems in Digital Signal Processing . . . . . 15
2.2.3.1 Aliasing . . . . . 15
2.2.3.2 Leakage . . . . . 15
2.2.3.3 Windowing . . . . . 15
2.2.3.4 Filtering . . . . . 16
2.2.3.1 Averaging . . . . . 16
2.3. Frequency Domain Identification . . . . . 16
3. INSTRUMENTED BUILDING . . . . . 18
3.1. Analyses Results . . . . . 24
4. FINITE ELEMENT MODEL . . . . . 28
4.1. Dimensions and Material Properties . . . . . 28
5. FEM Updating . . . . . 37

5.1. Error Function . . . . . 37
5.2. Matlab Code and Model Generation / Matlab – SAP2000 Integration . . . . 40
6. SEISMIC DEMAND . . . . . 43
7. CONCLUSION AND RECOMMENDATIONS . . . . . 57
REFERENCES . . . . . 61

# LIST OF FIGURES

Figure 3.1. The building monitored in project. . . . . 18

Figure 3.2. The residence complex and its location with respect to the bosphorus. . 19

Figure 3.3. Located sensors and receiver.. . . . . 20

Figure 3.4. Location of the accelerometers and the receiver.. . . . . 21

Figure 3.5. The plan view of the building. The locations and directions of the sensors inside the core are shown with arrows. The columns are highlighted. . . 22

Figure 3.6. TDG 6001 and Sensebox 7021.. . . . . 23

Figure 3.7. Representative ambient vibration data for the 5th floor in Y-direction. . 24

Figure 3.8. Representative ambient vibration data for the 26th floor in Y-direction. 24

Figure 3.9. Structural response in Y direction for all collected data. . . . . 25

Figure 3.10. Structural response in frequency domain in X direction. . . . . 25

Figure 3.11. Identified mode shapes in X direction. . . . . 26

Figure 3.12. Identified mode shapes in Y direction. . . . . 27

Figure 4.1. SAP2000 model of the building. . . . . 28

Figure 4.2. The view of shear wall core in the architectural drawings and in genuine. 30

Figure 4.3. Zoomed view of the core walls. . . . . 30

Figure 4.4. Mode shapes of the mathematical model in X direction. . . . . 34

Figure 4.5. Mode shapes of the mathematical model in Y direction. . . . . 35

Figure 5.1. FEM Updating Flowchart. . . . . 40

Figure 5.2. Error results of simulated combinations. . . . . 42

Figure 6.1. Marmara segment of North Anatolian Fault Zone and the location of the building. . . . . 44

Figure 6.2. Response spectra and several design code. . . . . 47

Figure 6.3. 2-directions interstory drift ratio time-history for Duzce, Turkey earthquake record. . . . . 49

Figure 6.4. 2-directions interstory drift ratio time-history for Kocaeli, Turkey (1) earthquake record. . . . . 49

Figure 6.5. 2-directions interstory drift ratio time-history for Northridge (2) earthquake record. . . . . 50

Figure 6.6. Maximum interstory drift ratio time-history of Kobe (2) record for 2% damping ratio. . . . . 51

Figure 6.7. Maximum interstory drift ratio time-history of Northridge (1) record for 2% damping ratio. . . . . 51

Figure 6.8. Maximum interstory drift ratio time-history of Imperial Valley (2) record for 2% damping ratio. . . . . 52

Figure 6.9. Maximum interstory drift ratio time-history of Loma Prieta (1) record for 2% damping ratio. . . . . 52

Figure 6.10. Maximum interstory drift ratio time-history of Northridge (1) record for 2% damping ratio. . . . . 53

Figure 6.11. Maximum interstory drift ratio time-history of Kobe (2) record for 2% damping ratio. . . . . 53

Figure 6.12. Maximum interstory drift ratio time-history of Landers (2) record for 2% damping ratio. . . . . 54

Figure 6.13. Maximum interstory drift ratio time-history of Imperial Valley (2) record for 2% damping ratio. . . . . 54

Figure 6.14. Probability density function of updated and non-updated maximum cases for drift ratio values. . . . . 55

# LIST OF TABLES

Table 4.1. Modal frequency comparison of fixed constraint modal and stick model. 29

Table 4.2. The effect of different modulus of elasticity of concrete values on the natural frequencies of model.. . . . . 32

Table 4.3. Frequencies of non-updated model with stick model of restraining effect and shell-elements in the core wall.. . . . . 33

Table 5.1. Frequency Comparison. . . . . 38

Table 6.1. Earthquake records. . . . . 44

Table 6.2. Maximum Interstory Drift Ratios. . . . . 50

Table 6.3. Results of Probability of Failure Analyses. . . . . 55

# LIST OF SYMBOLS

| | |
|---|---|
| *C50* | 50 MPa-class concrete |
| *E* | Modulus of elasticity |
| $E_{cj}$ | 28-day modulus of elasticity |
| *f* | Frequency |
| $f_{cj}$ | Compressive strength |
| *g* | Gravitational acceleration |
| *h* | Weighing coefficient for MAC value |
| *Hz* | Hertz |
| *k* | Weighing coefficient for modal frequency |
| *m* | meter |
| *km* | kilometer |
| *M* | Magnitude |
| *MPa* | Unitary matrix containing the singular vectors |
| *sec* | Second |
| | |
| *3G* | The third-generation of mobile telecommunications technology |
| *$2k* | Input file for SAP2000 software |
| $\psi$ | Mode shape |
| $\xi$ | Damping ratio |
| $\omega$ | Angular frequency |
| $\pi$ | Pi |

# LIST OF ACRONYMS / ABBREVIATIONS

| | |
|---|---|
| *ACI* | American Concrete Institute |
| *dir.* | Direction |
| *FE* | Finite element |
| *FEM* | Finite element model |
| *FDD* | Frequency domain decomposition |
| *GPS* | Global positioning system |
| *LVDT* | Linear variable differential transformer |
| *MAC* | Modal assurance criteria |
| *MEMS* | Microelectromechanical systems |
| *NAFZ* | North Anatolian Fault Zone |
| *nees* | Network for Earthquake Engineering Simulation |
| *PEER* | Pacific Earthquake Engineering Research Center |
| *PGA* | Peak ground acceleration |
| *SHM* | Structural health monitoring |
| *TBI* | Tall Buildings Initiative |
| *TDG* | Teknik Destek Grubu |
| *TS* | Turkish Standards |
| *UCLA* | University of California, Los Angeles |
| *USB* | Universal serial bus |

# 1. INTRODUCTION

## 1.1. Overview

Tall buildings are the foremost state-of-the-art examples of today's civil engineering world. Demand of sheltering created by increasing population of the world is naturally supplied by tall buildings while the diminishing of construction areas is inevitable. Tall buildings also represent a symbolic value of technology and success for the owner, as they supply more housing opportunities in a limited area, and, therefore, offer a more economical option in the areas where the construction areas are limited. Today, rapid technological developments satisfy the requirements of the race for construction of tall buildings. In the last decades, many tall buildings lost their title as "the tallest building in the world" in a very short time, and construction of new tall buildings increases rapidly.

As the need for housing is increasing in many countries and cities, certainly, more tall buildings will be constructed. However, especially in earthquake prone areas, taller buildings are prone to more serious risks than simple residency buildings. These risks can mainly be divided into two categories: first, earthquake vulnerability of the tall buildings which have been built in seismically active zones, second the condition of old tall buildings which may be affected by fatigue over the years. Both of the risk categories may cause significant economic losses, and even worse, they may lead to loss of human lives. In order to prevent such hazardous events it is essential to use all possible structural and earthquake engineering tools.

In the case of earthquake performance of a tall building, a limited extent of damage is allowed for economic reasons. However, in order to investigate the possible condition of a tall building after an earthquake that is, whether the building will be declared to be safe or not, a detailed simulation of the mathematical model is required for the building under several scenarios. On the other hand, as there are many uncertainties which are followed by numerous assumptions about the real building; it might not be very accurate to estimate the possible condition of the structure after an earthquake. Moreover, in the case of the

evaluation of an existing structure, there are many unknowns and again assumptions following that in order to give an exact idea about the structure. For instance, concrete core testing may not be representing the overall characteristics of the structure or the architectural drawings may not be exactly followed in the construction process. In contrast to theoretical and limited knowledge about the structures, structural health monitoring (SHM) provides experimental information which reflects the dynamic characteristics of the real structure. In both present condition evaluation of the structure and damage simulation of the structure in a possible earthquake, the dynamic characteristics of the building are very important for getting realistic results. For instance, damage detection can be applied via system identification techniques as a quantitative and a rather quick method.

Istanbul is a perfect example of a growing metropolis with very limited construction areas. It is also an earthquake prone city where pre-and-post cautionary measures for an earthquake hazard are not considered seriously. SHM techniques are used to understand existing conditions of structures, as well as their post-earthquake conditions. In order to investigate possible solutions to such necessities, in this study, a twenty-six story, core-wall tall building in Istanbul is instrumented with sixteen accelerometers. Natural frequencies and modal shapes of the building are obtained by frequency domain decomposition method. These results are compared with the modal values obtained from the finite element model of the building created according to design drawings and a finite element modal updating process is applied to the finite element model. Time history analyses under probable earthquake input motions are performed with that updated model. The study shows that model updating based on identified modal values is significant in the determination of seismic demands on tall buildings.

## 1.2. Literature Review

Structural health monitoring (SHM) is applied successfully in structural and earthquake engineering world as an objective and advanced technology method. Remarkable studies have been proposed related with this discipline. SHM is based on analyzing the data acquired by accelerometers on a structure, using identification techniques. System identification can be applied in time or frequency domain. SHM or

damage detection of a structure can be realized by the examination of modal parameters. System identification has been carried out in civil engineering from the early 1980s. Beck and Jennings (1980) suggested a work that structure is analyzed as a linear system and the modal parameters of this system are obtained in time or frequency domain.

Yun and Shinozuka (1980) introduced nonlinear identification of dynamic systems. Synthetic inputs and outputs are analyzed in order to test the success of the suggested methodology. It is found out that the performance of the methods is considerably well. On the other hand, these methods are found out to be inefficient by terms of computational efforts given. Ghanem and Shinozuka (1995) extended these works and gave several examples for system identification in structural systems.

Safak (1991) suggested a discrete-time method for system identification by using discrete-time linear filters as all the recordings taken are in the discrete form. Discrete-time relationship between the input and the output is shown via a discrete transfer function by several methods. Several points on data processing, model selection and model validation are explained with examples.

Lus *et al.* (1999), used earthquake inputs as excitation resources in order to measure the response for the system identification technique they offered. In this study multi-degree of freedom systems are identified and their dynamic properties are found. In order to that, Eigensystem Realization Algorithm and Observer/Kalman Filter Identification are used. These methods are tested on real world examples such as responses of an eight story building and a bridge to real earthquake records.

In order to obtain modal values, ambient vibration test or forced vibration tests may be used. In properly instrumented structures, modal parameters such as natural frequencies, mode shapes or damping ratios of the structure can be obtained using relevant analyses. In the case of the structural retrofitting of the structures, the effect of the retrofitting can be seen via simulations on a finite element model. Soyoz *et al.* (2012), made an ambient vibration survey on a building that structural retrofitting is applied. Moreover, a forced vibration test is applied beside ambient vibration survey. Following the instrumentation of

the building, enhanced frequency domain decomposition method is applied in order to obtain natural frequencies and damping ratio of the building. The effects of the retrofitting are investigated via FEM of the building.

In the case of long-term continuous monitoring projects, collected data can be processed via different algorithms and then a mathematical model of the building can be created and updated according to these data in order to simulate the behavior of the building in an earthquake. Wallace *et al.* (2006), undertake an ambient and low-amplitude earthquake vibration survey of a 15-story steel moment-frame building located in UCLA campus. This study successfully implements identification technics in order to identify the modal parameters of the first nine modes of the building. An initial FE model is created and updated using a modal-sensitivity-based method with parameters representing the additional mass and stiffness of the building that are not readily modeled.

Another research area can be soil-structure interaction which focuses on the effects of earthquake on the site soil and the differences in the earthquake waves when they reach to the structure. Kohler *et al.* (2005), proposed a study that Fourier amplitude spectra have been calculated from several intervals of ambient vibrations that are measured. Fourier amplitude spectra have been calculated from several intervals of ambient vibrations, a 24-hour period of strong winds, and from Encino, Yorba Linda and Central Alaska earthquakes. It is found that softening of the soil-structure system increases as amplitudes become larger. Moreover the change in frequencies revert to pre-earthquake levels within five minutes of the Yorba Linda earthquake where the first shear wave recorded takes about 0.4 sec to travel up the 17-story building. Lastly, it is reported that shaking due to strong winds that occurred during the Encino earthquake dominates the frequency decrease, which correlates in time with the duration of the strong winds.

Furthermore, interstory drift ratios which are used as a performance measurement can also be obtained via accelerometer data in non-linear systems as well as linear systems if proper instrumentation techniques are used. Wallace (2010), proposed a study on a four-story reinforced concrete building. A forced vibration test is applied utilizing the nees@UCLA Mobile Field Laboratory. Importance of the proper instrumentation is

emphasized as it is observed that LVDT may not be the best option compared to non-contact sensors. Furthermore, very common assumptions which are used in design procedures that the diaphragm could be assumed to be rigid and that soil-structure-foundation-interaction was insignificant could be verified.

SHM systems are applied on ordinary buildings, bridges and also on tall buildings. As an example, investigation of earthquake responses of tall buildings using system identification techniques can be given. Celebi and Safak (1991), Celebi and Safak (1992), introduced studies discrete time linear filtering methodology with least-squares approximation and assumption of a multi-input, single-output model for the building is used for system identification. It is shown that effect of higher modes and the rocking phenomena are significant in tall buildings.

SHM methods are also used to evaluate the performance of tall buildings during earthquakes. It is shown that, interstory drift ratios can be obtained from the collected acceleration data. Celebi *et al.* (2004), proposed an advanced seismic monitoring system for a 24-story building. This system offers the rapid evaluation of a building in a post-earthquake situation. Collected acceleration data is used as a measure of damage by means of interstory drift ratios. In these studies, finite element modeling of the structure has a significant role, in particular, modeling of the shear walls and the frame elements in tall buildings. Wallace (2007), offers an overview of modeling approaches. In this study, modeling of both flexural and shear responses with the potential impact of coupled flexure–shear behavior are investigated. Based on the findings, valuable specific recommendations are made for general modeling issues.

When applying SHM methods, it should be noted that changes in modal parameters may also be changed about + 10% due to environmental effects, such as temperature, rather than due to damage in the structure. This can be observed in the study introduced by Soyoz and Feng (2009), which is a 5-year monitoring project for a bridge with identification applications. The same phenomena is pointed out by Yuen and Kuok (2010), in their project which daily measurement of a 22-storey reinforced concrete building is

utilized for one year to monitor the variation of its modal frequencies, which are identified using the Bayesian spectral density approach with the ambient vibration data.

In tall buildings, like all other structures, obtained modal parameters show differences between finite element model (FEM) and the experimental data. The main reason for that difference is the assumptions made in the finite element modeling such as in the modeling of in-fill walls. As a result, modal parameters obtained from collected data may be different than the assumptions made according to design codes. In a research undertaken by Guler *et al.* (2008), which uses data collected from six building in the construction phase, it is shown that in-fill walls have an effect on natural frequencies up to 20%.

Furthermore, Brownjohn *et al.* (2000), showed that FEMs with different designing detail result in different model parameters. In this study, different FEMs are used and the model parameters of these models are compared with the ones obtained from ambient vibration surveys. It is shown that increased detailing in modeling increases the accuracy in model parameters, while the simplest stick model is acceptable for the first translational modes. Moreover, for the torsional modes the core-wall detailing in modeling is very significant. Brownjohn (2003), also proposes two ambient vibration surveys in order to investigate the performance of two system identification technics, namely Natural Excitation Technic combined with eigensystem realization algorithm and Improved Peak Picking or as originally called frequency domain decomposition.

In order to minimize the errors caused by the assumptions made in FEM, the model is updated according to the data collected. General process is, first, creating an initial FEM based on the architectural drawings, and then, updating this model with the data collected using various methods. The new, more realistic model can be used to simulate the performance of the building in several conditions. This technique has been applied successfully to buildings, bridges and wind turbines. Jaishi and Ren (2005), present a practical and user-friendly finite element (FE) model updating technique for real structures using ambient vibration test results. Frequency residual only, mode shape related function only, modal flexibility residual only, and their combinations are studied independently. In

view of tuning as well as damage localization, offered full objective function is found to be the best for FEM updating. Hartmann *et al.* (2011), established a study on wind turbines in order to estimate their probabilistic lifetimes. Following FE analyses, operational mode analyses are run using enhanced frequency domain decomposition and stochastic subspace identification. This work successfully couples sensor-based structural health monitoring with finite element model updating for probabilistic-based lifetime estimation.

Performance and reliability of the structures can be expressed in terms of fragility curves or similarly probability density functions in case of earthquakes and tornados. Following a realistic FEM, different earthquake or tornado scenarios can be simulated in order to measure the response of the structure under these loadings in a probabilistic way. Therefore performance of the building can be foreseen in terms of damage levels. Following that, an approximate lost and renewal calculation can be made. Jayaram *et al.* (2012), introduced a systematic simulation approach based on the PEER loss assessment framework is used to develop building vulnerability functions that provide estimates of losses to buildings underground motions of various intensities. Emphasis is placed on capturing the effects of epistemic and uncertainties in random variables, such as ground motions, structural response parameters etc., to quantify the uncertainty in the final loss estimate. As there are several methods available in the literature, simpler methods have been suggested for the linear responses of the structures, while for the non-linear response of the structures more complex methods have been proposed.

Tantala and Deodatis (2002), offered a methodology in order to develop seismic fragility curves for tall buildings. Monte Carlo simulations are used to define the uncertainties in the ground motions and the structural characteristics. P. Guéguen *et al.* (2012), introduced behavior models for each class of structure for vulnerability assessment by using ambient vibration. Both a methodology of multi-degree-of-freedom system including higher modes and methodology of a simple single freedom system with the fundamental mode are used to build fragility curves. Moreover, by introducing the experimental modal model of the buildings, it is proposed to improve seismic risk assessment at an overall scale (the city) or a local scale (the building) for the first damage grade (slight damage).

It is also reported that in tall buildings, the general damping ratio estimation for the reinforced concrete buildings is not realistic. In several studies, it is shown that 5% damping ratio is not appropriate for the tall buildings as it is more than the real value. Boroschek and Yanez (2000), proposed a study that dynamic properties and response characteristics of a 22-stories high structural wall Chilean building are identified using parametric and nonparametric system identification techniques. In order to do that a series of strong motion and ambient vibration records have been obtained. Typical values for critical damping ratios are found out to be between 1 and 2%.

Satake *et al.* (2003), showed that the first damping ratio is inversely proportional with the building height as well as vibration amplitude and foundation type. Furthermore, the damping ratios are generally higher in hotels and apartments which have more interior partitions than those of other buildings. The higher-mode damping property is reported to be intermediate between the stiffness-proportional type and the invariable type. The ratios of two adjacent mode damping ratios and damping ratio predictors are also proposed. Smith *et al.* (2010), showed that, in the buildings that is above 250m, damping ratios are found out to be unconservative. There is no measurement of damping ratio above 1% for these buildings. A higher damping ratio estimation will lead to the calculation of lower seismic demand on the building. For instance, if the damping ratio is taken as 0.8% rather than 2%, the response of the building will be increased by 50%. Several other serviceability problems are also pointed out in the case of lower or uncertain damping.

Wind effects on the building have been investigated so far. As an example for dynamic loading on a tall building, literature on wind induced response of tall buildings is investigated in this study as well. For instance, it is shown that in the case of an assumption of higher damping ratio on a building, the response of the building will be calculated to be lower than the real values. This miscalculation can lead to unexpected damage or accelerated fatigue. SHM program has been established in order to investigate the response of tall buildings under wind loads in Chicago, USA [Kijewski-Correa and Pirnia (2007)]. The authors also introduce their experiences about the buildings in Boston and Seoul. In particular, this study focuses on the effects of coupling, beat phenomenon, amplitude dependence, and structural system type on dynamic properties, as well as correlating

observed periods of vibration against finite element predictions. Results show that damping ratio is increasing with the excitation amplitude. Moreover, the increased energy dissipation and amplitude dependence of buildings characterized by frame action, indicating that features of the structural system type are equally central to any viable prescriptive damping standard. Kijewski-Correa *et al.* (2006), also show the possibility of usage GPS in monitoring the dynamic responses of tall buildings under wind loading. In GPS tracking is superior in lower frequencies with errors less than 10% which makes GPS more suitable for civil structures. Research done on this subject are improving the design methods for the wind-resistance and high performance buildings as they are also clarifying the unknowns in the behavior and the modal parameters of tall buildings

Q.S. Li *et al.* (2000) and Q.S. Li *et al.* (2003), show that at relatively low amplitudes, the effective stiffness may be significantly higher due to contributions from non-structural components. Furthermore, the measured damping demonstrates amplitude-dependent characteristics and increases with increasing amplitude. There is a wide range of studies in terms of experimental data from wind-tunnel tests to real-time typhoon cases which makes them more valid in terms of the selection of very different cases in order to show the response of tall buildings for such different cases. Q.S. Li *et al.* (2006), also introduced that damping values of 0.5%–1.0% of critical appeared reasonable for wind-resistant design of super tall buildings for serviceability consider. Moreover it is shown in this study that the field measurements of acceleration data were consistent with those obtained in the force balance model study in the wind-tunnel testing.

### 1.3. Objective

In Istanbul, a mega city with a population of 15 million, construction areas are very limited. As a result of that, tall buildings have been constructed rapidly in the last decade. However, the Turkish Design Code is very limited for designing tall buildings. Therefore, a better understanding of the behavior of the tall buildings is required in order to make more realistic assumptions in the design process. SHM and system identification techniques are very useful for collecting knowledge about the behavior of the constructed

buildings and will lead to a better understanding of tall buildings and, therefore, to better designs.

SHM and system identification methods are widely used in order to evaluate the performance level of structures with a high level of confidence. Istanbul, as a city with many old, not well-designed buildings, is very vulnerable to severe earthquakes. Therefore, in the case of a very likely event of an earthquake in Istanbul, SHM and system identification techniques can be used very effectively in order to understand the current situation of the structures.

Therefore, in order to meet these needs, this study investigates the application of a whole SHM project. From the beginning to the end, an SHM project is applied to a tall building, providing valuable experiences for the design philosophy of tall buildings and for the evaluation practices of a huge structure after a possible earthquake.

In this study, first, installments and data acquisition is completed. Afterwards, system identification is applied via frequency domain decomposition method. Modal parameters such as natural frequencies and mode shapes are obtained. Following that a FEM is created according to drawings. Several modeling alternatives are applied and compared. A FEM updating code is run in order to update the mathematical model as close as possible to the real building. Finally, seismic demand analyses are performed in order to see the performance of the building in a possible earthquake which is caused by North Anatolian Fault. A probability density function for different cases established in order to find the probability of failure under simulated ground motions.

### 1.4. Scope of the Study

This study is structured according to the order of the procedures in the project. In chapter 1, the motivation of the study, a thorough literature review, the objectives of the study and the scope of the project are presented.

In Chapter 2, the system identification process is explained along with a brief introduction to the digital signal processing. Moreover, in this chapter, the frequency domain decomposition method is presented as well. The chapter covers the theoretical base of the system identification process.

Chapter 3 introduces an instrumented building. The building itself, the location of the building, instrumentation of the building and the instruments are introduced in this chapter as well. The outcomes obtained from this instrumentation process are presented.

In Chapter 4, the finite element model is described in detail. Different modeling techniques and the comparison of these techniques are discussed. The mathematical models and the results obtained from these models are presented.

Chapter 5 explains the FEM updating process. The Matlab code used in the analysis, the integration of the Matlab code and the FEM software and its working philosophy are discussed. The error function used for selecting the best combination is presented as well. The results of the study are also indicated.

In Chapter 6, the seismic demand on the building is calculated and presented. Brief information about the site and seismology of the area are provided. The methodology that has been followed for the selection of the earthquake records, the effect of different damping ratios, results of time-history analyses for non-updated and updates cases, comparison of these results and finally the probability of failure of the building according to these records are expressed in terms of probability density functions.

Finally, conclusion is represented in Chapter 7, which includes the findings of this study. The results of analyses, comments on them and possible future work are discussed.

# 2. SYSTEM IDENTIFICATION

## 2.1. General

System Identification methods can be categorized as time domain or frequency domain methods by means of the base they are investigated on. Moreover, another categorization can be made as input-output methods or output only methods.

In input-output methods which are generally as used in the analyses of the response of a system under a forcing function such as earthquakes, the response obtained includes both the structural behavior and the excitation content. Therefore it is needed to cancel out the effect of excitation source in the response obtained.

On the other hand, in the output-only methods, such as ambient vibration surveys, there is a very low amplitude and broad band frequency content in the input ground motions which are created naturally via “ambient” sources. In experimental cases, this kind of inputs can be represented by a function called “White Noise” which has a constant frequency content which does not interfere in response signal with any predominant frequency.

In this study, system identification is carried out in frequency domain and as an output-only method. Several data are collected and processed with digital signal processing techniques in order to get modal parameters of the building. Measurements taken are ambient vibration measurements which are low amplitude and they are used for system identification process, namely frequency domain decomposition, (FDD) in order to get modal parameters of the system. In this section, digital signal processing and FDD techniques will be examined. Finally, results of the analyses will be presented.

## 2.2. Digital Signal Processing

### 2.2.1. Signals in Time Domain

Signals can be considered as a function composed of series of periodic functions. This periodicity could be represented by sinusoidal and cosinusoidal functions which have different amplitudes and frequencies. Thus, signals can be represented by Fourier series shown in the Equation 2.1 such as

$$x(t) = \frac{a_0}{2} + \sum_{n=1}^{\infty} \left( a_n . cos\left(\frac{2.\pi.n.t}{T}\right) + b_n . sin\left(\frac{2.\pi.n.t}{T}\right) \right) \tag{2.1}$$

Where t is time, T is period, $a_0$, $a_n$ and $b_n$ are components defined in Equation 2.2, Equation 2.3 and Equation 2.4.

$$a_0 = \left(\frac{2}{T}\right) \int_0^T x(t).dt \tag{2.2}$$

$$a_n = \left(\frac{2}{T}\right) \int_0^T x(t).\cos\left(\frac{2.\pi.n.t}{T}\right).dt \tag{2.3}$$

$$b_n = \left(\frac{2}{T}\right) \int_0^T x(t).\sin\left(\frac{2.\pi.n.t}{T}\right).dt \tag{2.4}$$

For computational purposes, a discretized form of Fourier series is more suitable as data is obtained in digital format. In order to get a discretized version of the function interested which has N number of step Equation 2.5 can be used such as

$$x(t_k) = \frac{a_0}{2} + \sum_{n=1}^{N/2} \left( a_n . cos\left(\frac{2.\pi.n.k}{N}\right) + b_n . sin\left(\frac{2.\pi.n.k}{N}\right) \right) \tag{2.5}$$

where $a_0$, $a_n$ and $b_n$ components are defined by Equation 2.6, Equation 2.7 and Equation 2.8.

$$a_0 = \left(\frac{2}{n}\right).\sum_{k=1}^{N} X_k \tag{2.6}$$

$$a_n = \left(\frac{1}{N}\right).\sum_{k=1}^{N} X_k.cos\left(\frac{2.\pi.n.k}{K}\right) \tag{2.7}$$

$$b_n = \left(\frac{1}{N}\right).\sum_{k=1}^{N} X_k.sin\left(\frac{2.\pi.n.k}{K}\right) \tag{2.8}$$

### 2.2.2. Cross Power Spectral Density

Spectral values of a signal can be expressed as a function of frequency and it is called as Power spectral density. The term “power” is used as square value of spectral density of a signal. Power spectral density obtained from an output is the response of the system under a dynamic loading. From such response data, frequency domain information can be obtained as it reflects both the input excitation and the behavior of the system. In ambient vibration case, with low amplitude and broad band frequency content, input is not expected in predominant frequencies in response function. Therefore, response data obtained from the structure are directly in terms of structural response of system.

In Matlab code used, csd Matlab code is used (It is replaced by cpsd code in subsequent updates. Csd code is still applicable for the same usage.). This code is applied with a resolution of 4096 data point, 500 Hz sampling frequency, a Hanning window filter and an averaging number as shown below.

Cyy=csd(data(:,isensor),data(:,jsensor),num_FFT,sampling_freq,hanning(num_FFT),num_averaging);

Where Cyy represents the power spectral density, data represents the collected data, num_FFT represents the resolution applied, sampling_freq represents the sampling frequency, hanning(num_FFT) represents the Hanning window for the applied resolution and num_averaging represents the averaging number.

These sections in the code described above are used to cancel out some digital signal processing problems. For instance sampling frequency is selected accordingly in order to prevent aliasing, windowing is selected in order to prevent leakage etc. These problems are described in detail below.

### 2.2.3. Problems in Digital Signal Processing

Measurements taken are digital data that is transformed from analog data which means, digital data is the discretized version of analog data. If required precautions are not taken in signal processing procedure, the outcomes of the analyses will not be accurate. Therefore, some of the problems are discussed and considered.

2.2.3.1. Aliasing. In case of signal converting from analog to digital, improper sampling rate can result in aliasing. In this phenomenon, if sampling rate is not sufficiently high some data points may be missed therefore the result is different than the expected. As a result, all the work done on this data will also have errors. The sampling frequency is taken as 500 Hz in this study which can cover signals up to 250 Hz. As the natural frequencies observed from system identification process are up to about 6.6 Hz, the sampling frequency is sufficient to cover these low frequencies (Ewins, 2000).

2.2.3.2. Leakage. In data acquisition, signal has to be taken for a finite time length of time. Together with this limitation, assumption of periodicity of signal may not hold for all cases. In such a situation the single frequency which the original time history has cannot be indicated. Energy “leaked” into several spectral lines around the true frequency and the spectrum can be seen over several lines or windows (Ewins, 2000).

2.2.3.3. Windowing. Windowing has several benefits for several problems on digital

signal processing such as introducing significant improvement on leakage problem. Windows are generally applied as time functions before applying Fourier transform to the signal. Some examples can be given as the Hanning window, which is used in this study, Cosine Taper window which can be used for random vibration or the Exponential window which can be useful for transient vibration applications (Ewins, 2000).

2.2.3.4. Filtering. Filtering is another digital signal processing tool like windowing, which helps reducing the noise level in the signals which can be caused by several reasons in recording process such as environmental or operational factors. As a result of the noise, signals may not reflect the real vibrational characteristics of the system. In order to prevent such a problem, filtering is used as a common noise reduction tool. Low-pass filters are commonly used in system identification of structures which generally have low level of natural frequencies (Ewins, 2000).

2.2.3.5. Averaging. Random vibration signals cannot be properly analyzed by Fourier transforms. In order to get spectral density estimations and correlation functions to characterize this type of signals, averaging is used as a tool to get better statistical reliability and less noise in the signal. This can be done by calculating discrete Fourier Transform in a very short time interval and following that overlapping and averaging the signal in that very short time interval (Ewins, 2000).

## 2.3. Frequency Domain Identification

Brincker *et al*. (2001), developed a frequency domain decomposition (FDD) technique which attempts to obtain modal parameters without the input data. In FDD method, outputs are transformed into frequency domain and create a series of square matrices which create a three dimensional matrix. In a given frequency, singular value decomposition of the square matrix at that frequency gives the spectral value and the mode shape at that frequency. Decomposition of spectral density matrix can be formulated as Equation 2.9.

$$S_{YY}(\omega) = U(\omega).\sum(\omega).U^{H}(\omega) \tag{2.9}$$

where $\sum(\omega)$ is diagonal matrix of the singular values, $U(\omega)$ is unitary matrix of the singular vectors and the superscript H denotes the complex conjugate and transpose.

Spectral values show the response of the system in frequency domain at that frequency. Therefore, even close modes can be obtained by fine discretization of frequency domain which provides of obtaining modal frequencies and mode shaped as well.

# 3. INSTRUMENTED BUILDING

A recently constructed tall building, shown in Figure 3.1, located in Zincirlikuyu, Istanbul has been temporarily instrumented.



Figure 3.1. The building monitored in project.

Permanent instrumentation is being carried out which will allow us to monitor the building continuously. The building is a part of residence complex with four towers and a shopping mall in the first five floors around the towers in addition of seven floors underground. Such a big structure can be quite complex to study within the scope of this research. Therefore, efforts are focused on one of the towers. The residence complex and its location with respect to the bosphorus can be seen as shown in Figure 3.2.

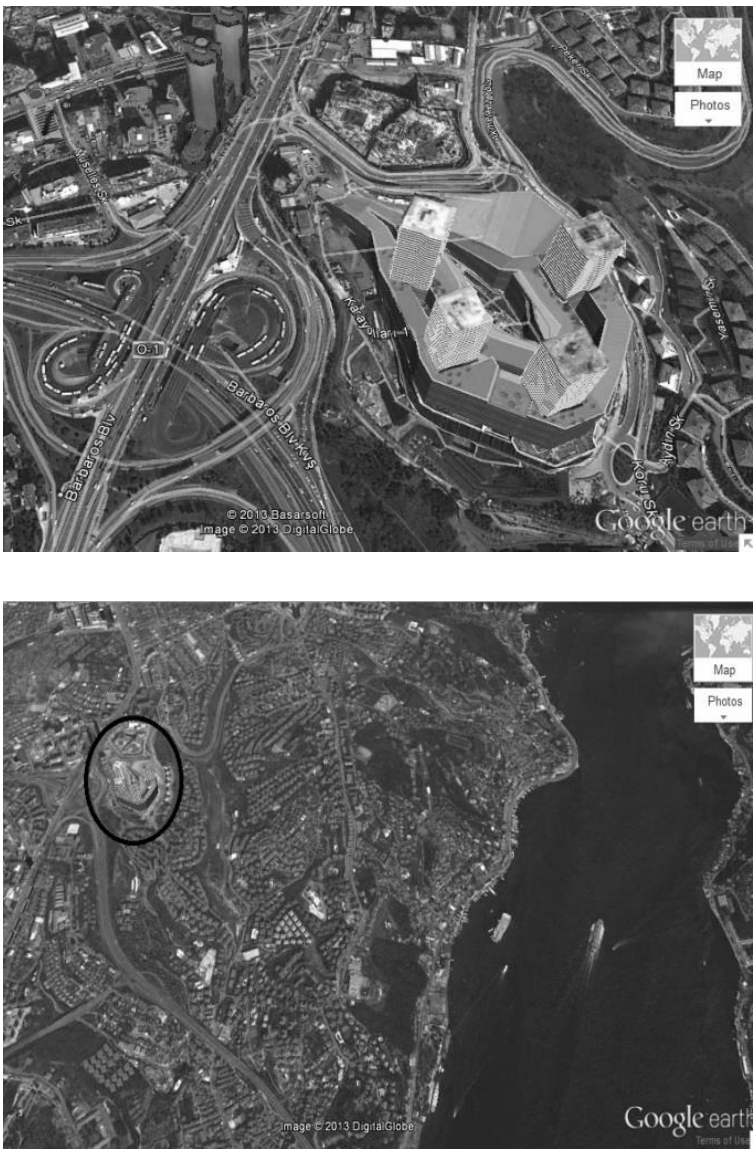


Figure 3.2. The residence complex and its location with respect to the Bosphorus.

Overall monitoring system consists of the receiver, the sensors and the cables connect these two to each other. The receiver is placed on 12th floor which is connected

via cables to all accelerometers. Locations for accelerometers are selected accordingly in order to be able to catch mode shapes as clear as possible. Five data cables for future sensors are installed at the foundation level in order to get possible earthquake excitations. For the first, fifth, twelfth and seventeenth floors, two sensors are placed in each floor. Finally for the twenty-sixth floor, three sensors are installed also to be able to get torsional modes. The receiver and sensors are shown in Figure 3.3. Their location is shown in Figure 3.4, Figure 3.5 and Figure 3.6.



Figure 3.3. Located sensors and receiver.

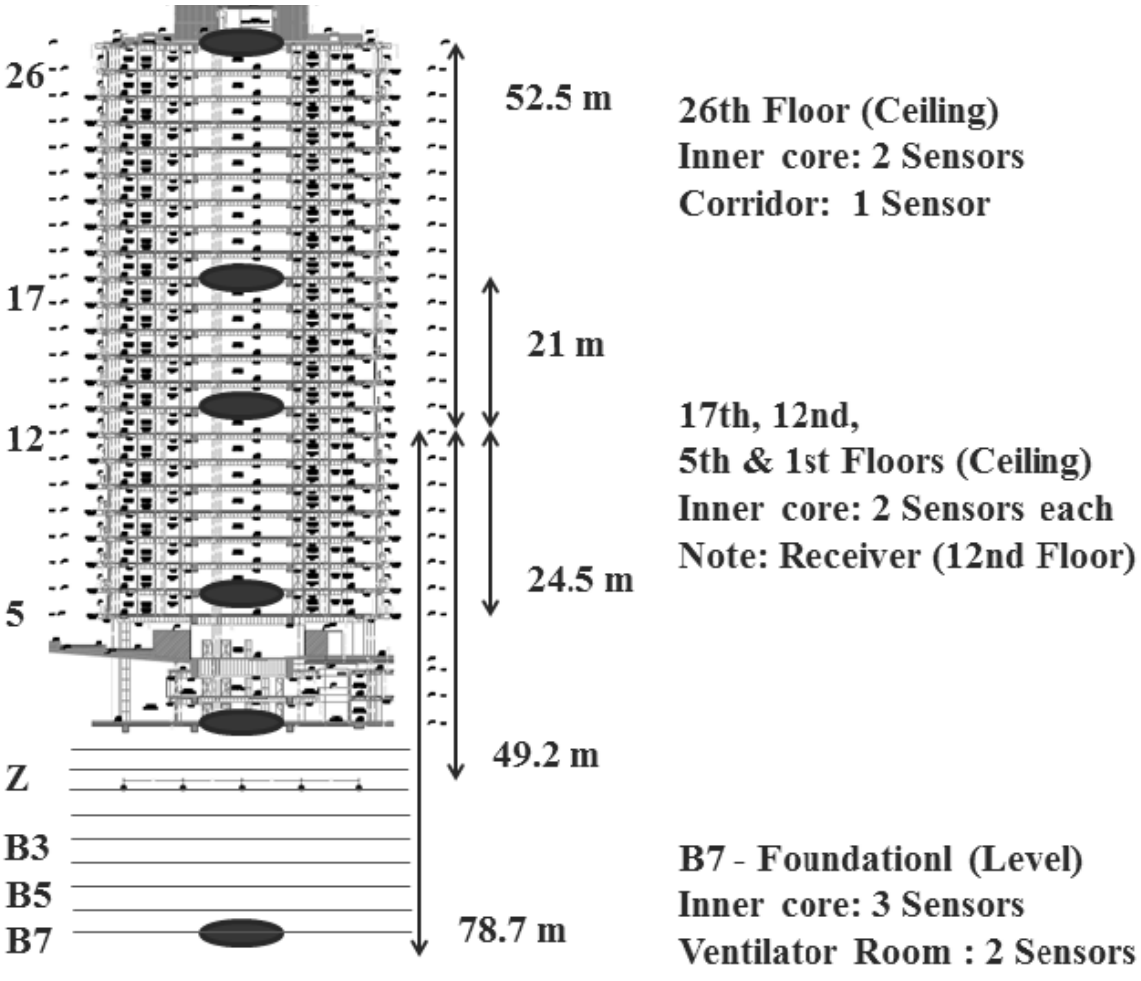


Figure 3.4. Location of the accelerometers and the receiver.

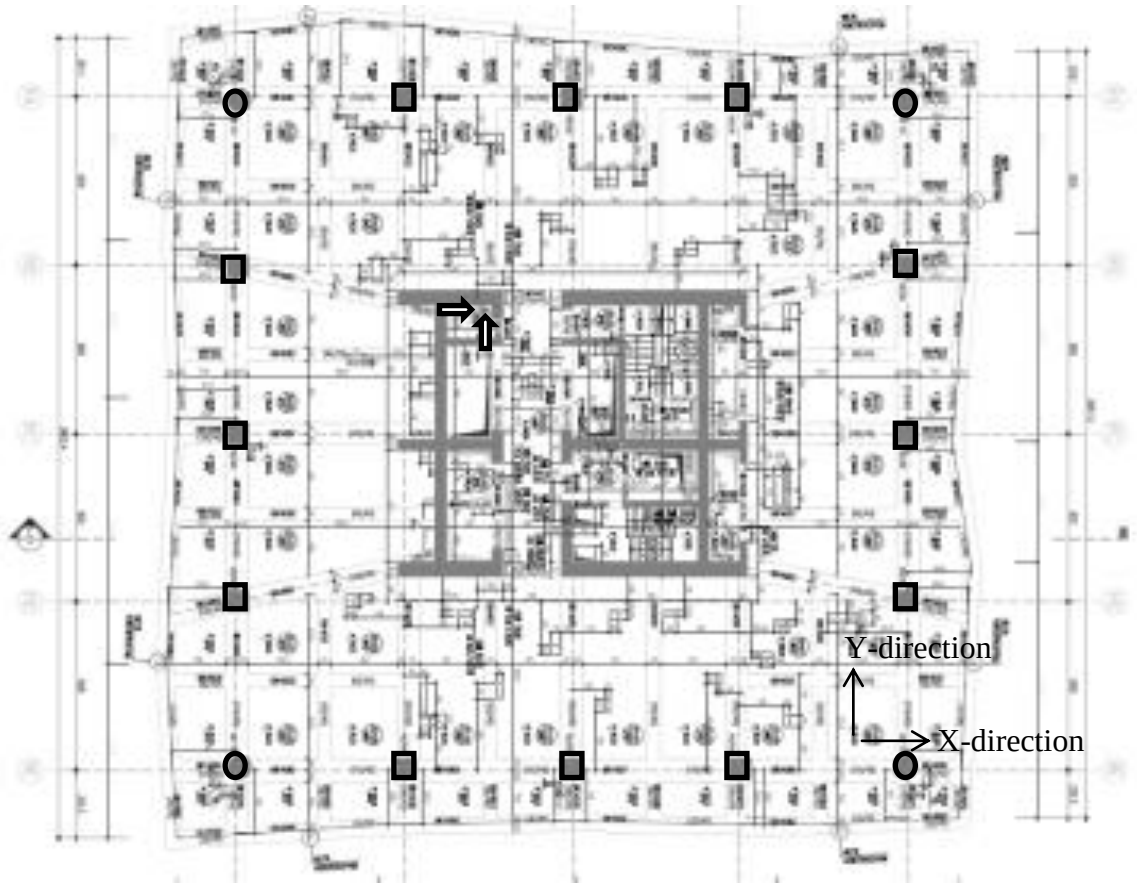


Figure 3.5. The plan view of the building. The locations and directions of the sensors inside the core are shown with arrows. The columns are highlighted.

As a receiver TDG Textbox2010 is used. It is a 16-channel dynamic data acquisition system which has an embedded netbook with software. It can collect data with up to 1000 Hz sampling frequency. TDG Sensebox accelerometers are used. These are micro electro mechanical system (MEMS) accelerometers which can perform between -3g and +3g excitations. The receiver and the sensors are shown in Figure 3.6.




Figure 3.6. TDG 6001 and Sensebox 7021.

Various laboratory tests are applied to the system in different sampling and recording frequencies. The importance of these tests should be noted in order to be sure about the reliability of the data. The condition of the data acquisition system directly affects the results of system identification analyses.

Accelerometers are placed at sixteen locations in the selected tower to measure vibration response with a sampling frequency of 500 Hz. Different sampling frequencies are also used to investigate the possible effects of sampling frequencies. It has been seen that there is no significant difference between 200 Hz and 500 Hz. Therefore, 500 Hz is selected as sampling frequency and the data collected in 500 Hz.

Lately, the system is turned online with the help of a USB modem that connects the system to the internet via 3G connection. That way, the system is available for remote control of the user from the office for all applications that system has, such that, data acquisition, setting up trigger system in order to start data acquisition in a desirable time for a desirable duration, transfer of this data etc. System is also capable of threshold triggering, which is starting data acquisition automatically if the acceleration values are higher than a pre-determined threshold value. This option is more suitable for the continuous health monitoring of the building in possible earthquake events.

### 3.1. Analyses Results

Figure 3.7 and Figure 3.8 show representative ambient vibration data taken from the 5th and 26th floor of the building, respectively.

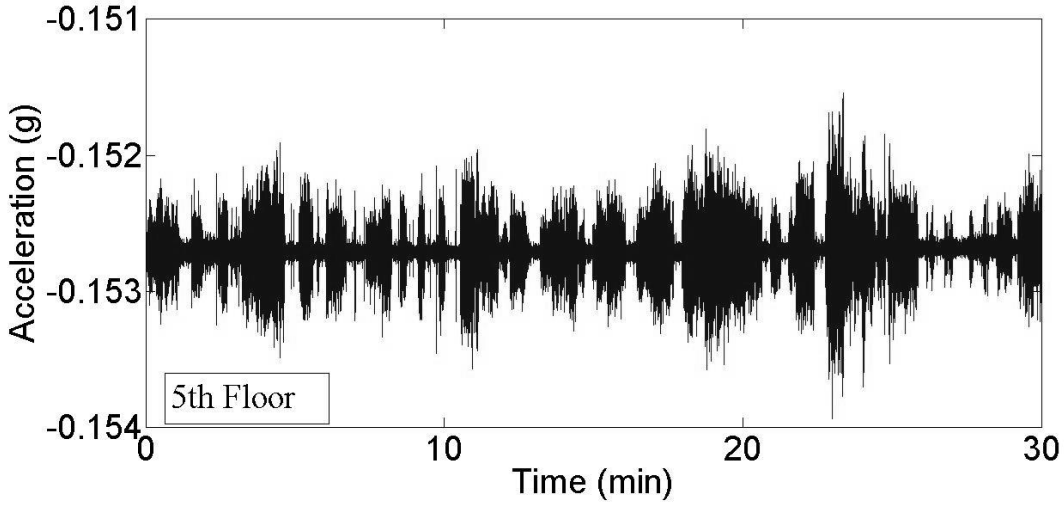


Figure 3.7. Representative ambient vibration data for the 5th floor in Y-direction.

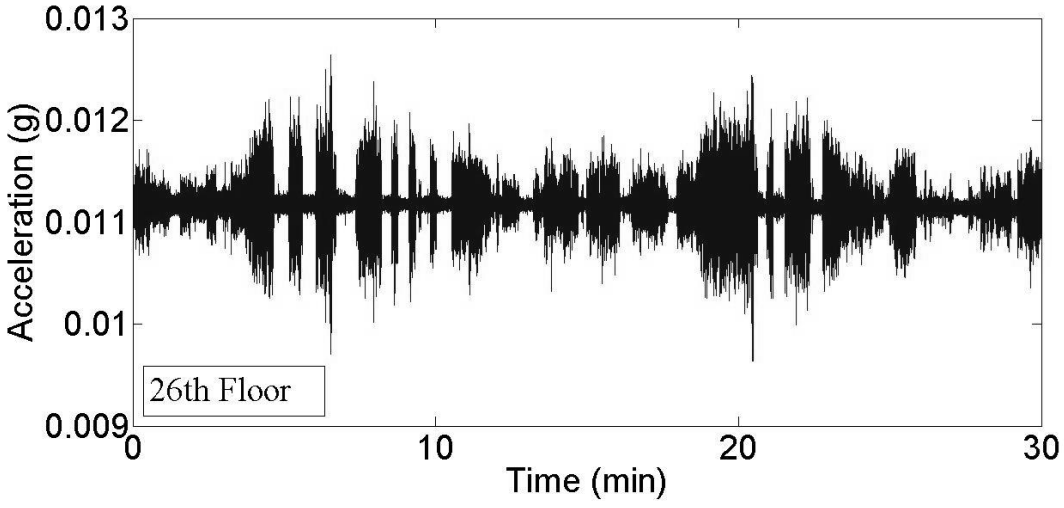


Figure 3.8. Representative ambient vibration data for the 26th floor in Y-direction.

Following the data acquisition, vibration response is analyzed by FDD method which is carried out via Matlab platform to obtain modal frequencies and mode shapes of the structure. Figure 3.9 shows the all data collected in Y-direction in order to express the

stable modes while Figure 3.10 shows the first singular values in the frequency domain in the X-direction for a selected record.

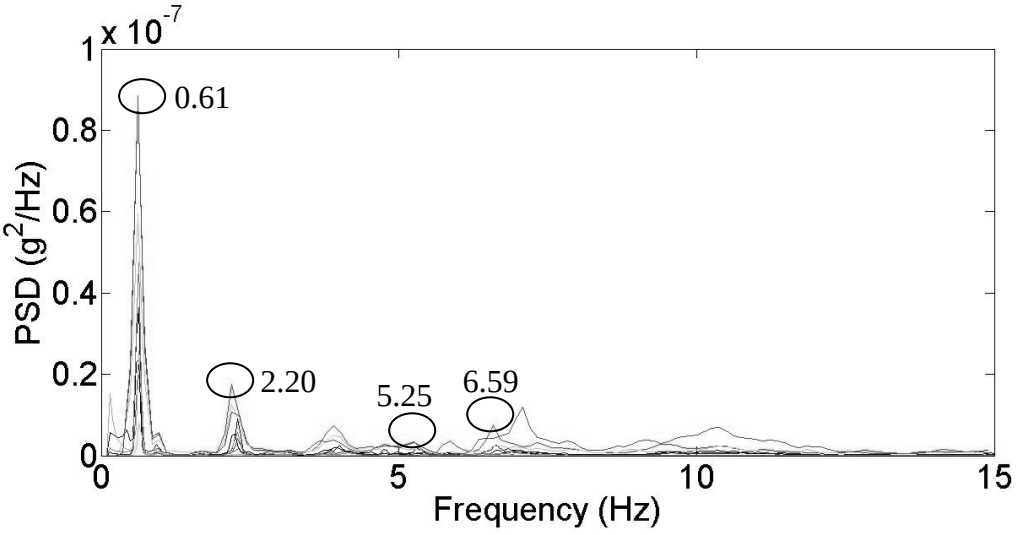


Figure 3.9. Structural response in Y direction for all collected data.

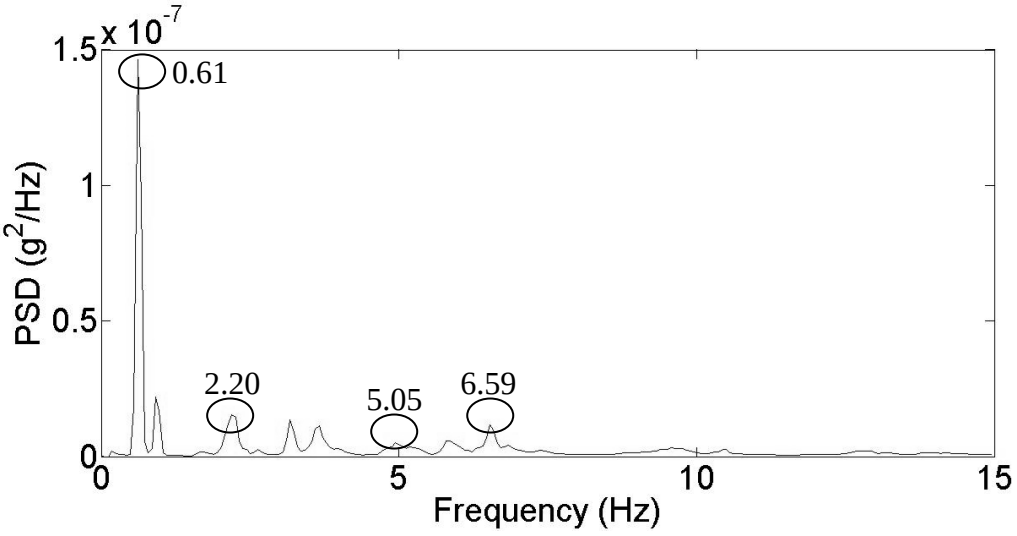


Figure 3.10. Structural response in frequency domain in X direction.

The peaks in this figure represent the structural modal values. From additional data acquisitions, it is found out that there is a torsional mode at 0.97 Hz. Only peak that could not be identified is the one around 3 Hz. At this frequency, mode shape obtained is very similar to the third mode, which is identified as at 5.249 Hz. These values are obtained from a set of data that is collected throughout a significant time to check the possible

natural frequency changes over time. In order to that, early morning and evening data are also collected to check the effect of temperature change on the natural frequencies. In these data, there is no difference in terms of natural frequencies in the time interval of data collection. However, it is believed that as long as data collected long enough the changes in the natural frequencies of the system due to environmental effects will be obtained. The first four mode shapes are also presented for the X direction in Figure 3.11 and for the Y direction in Figure 3.12.

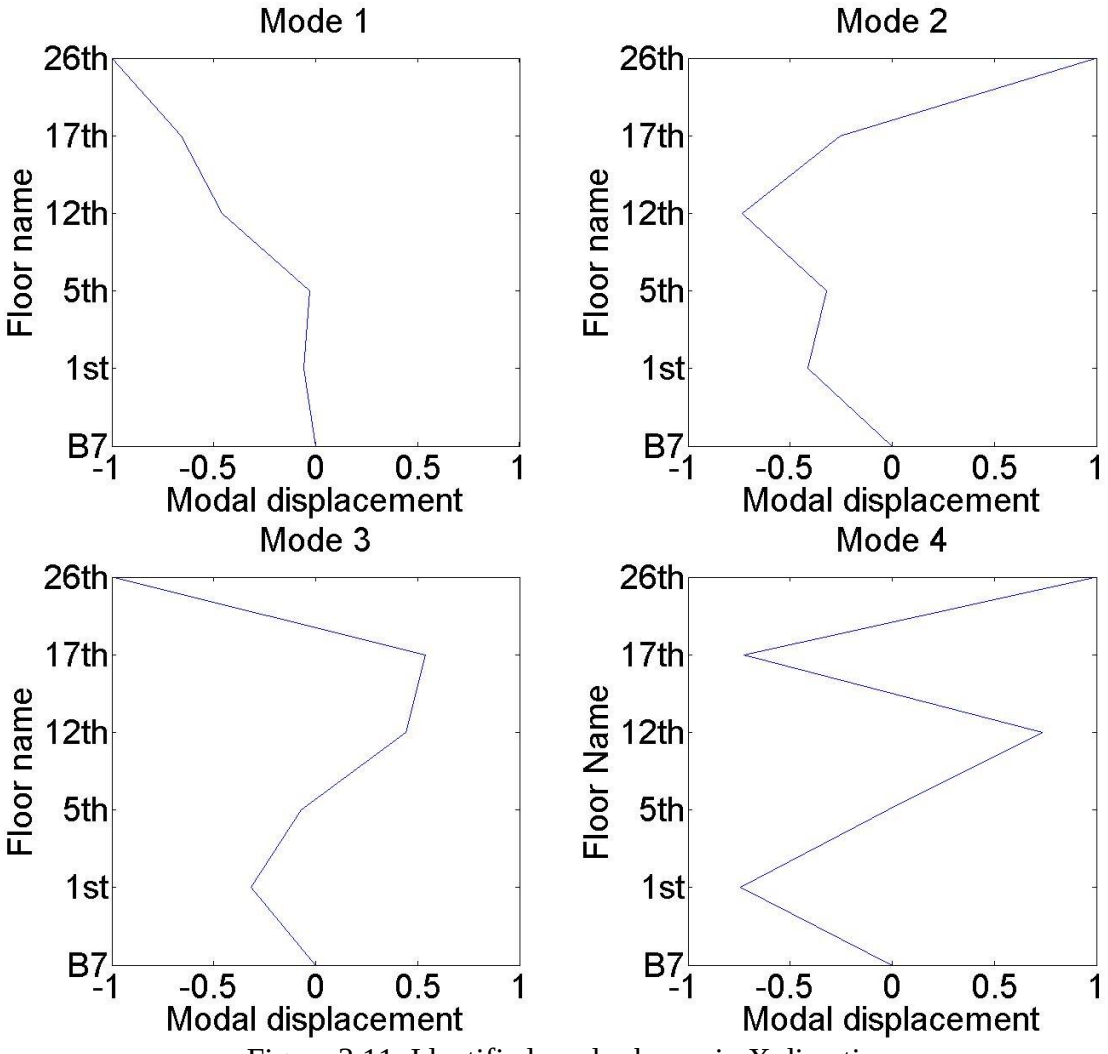


Figure 3.11. Identified mode shapes in X direction.

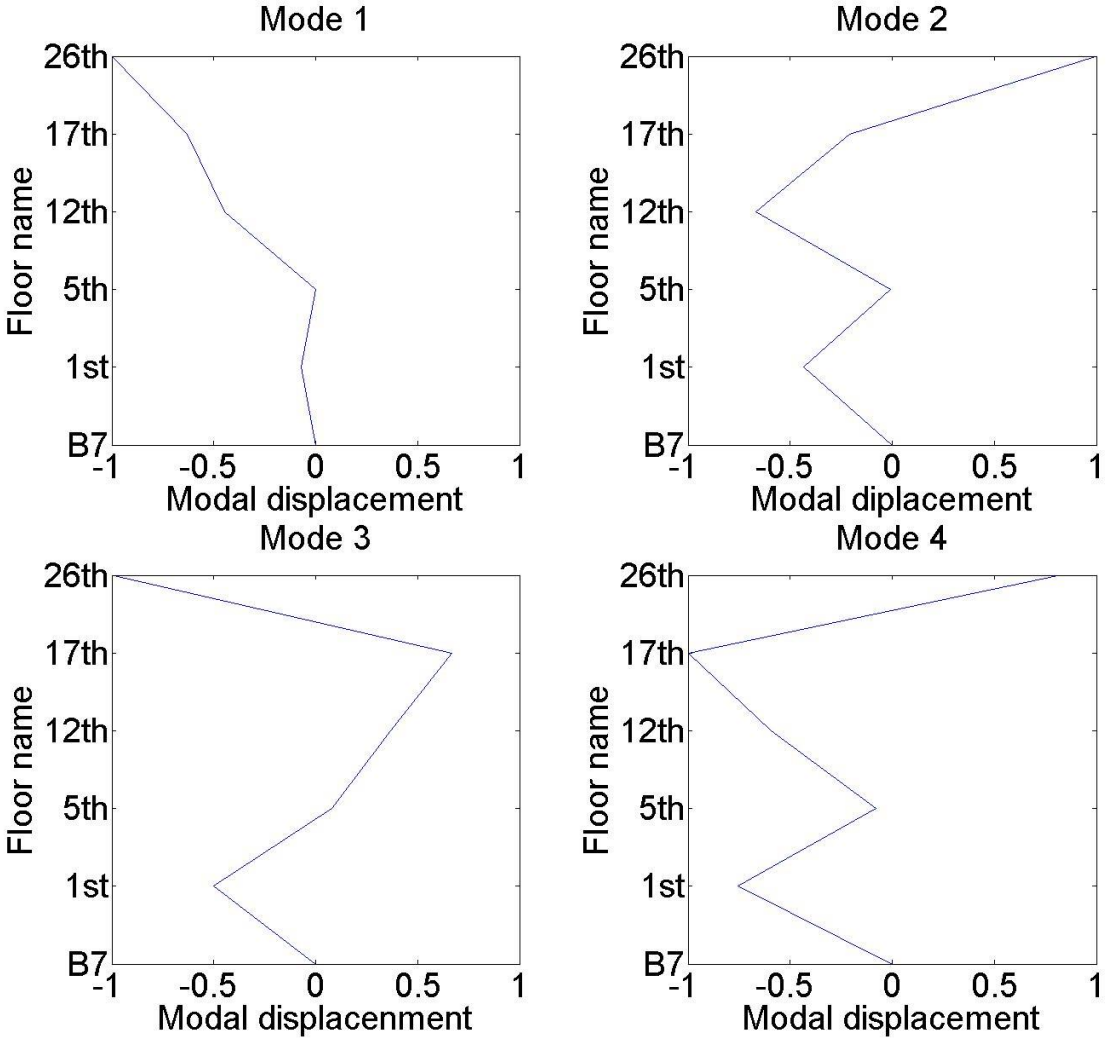


Figure 3.12. Identified mode shapes in Y direction.

# 4. FINITE ELEMENT MODEL

## 4.1. Dimensions and Material Properties

In addition to experimental determination, modal values were also obtained analytically. Architectural drawings are used in finite element modeling of the building. The mathematical model is created by SAP2000 v15.1.0 Ultimate Software as shown in Figure 4.1.

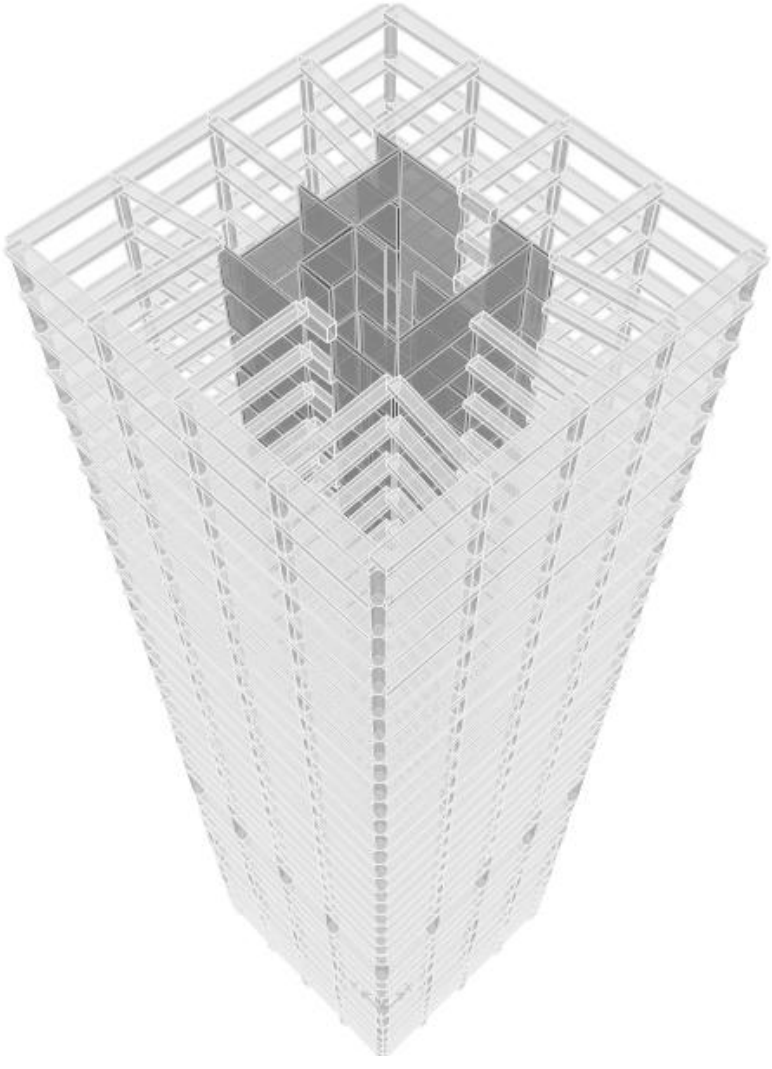

Figure 4.1. Sap2000 model of the building.

Building investigated has a 34 floors in total (7 floors underground and 27 floors above ground.). In the real building there is also a shopping mall which is a wider structure in the first five floors around the tower. For the sake of simplicity this part is not modeled explicitly but represented with a stick element which contributes to the lateral stiffness representing the shopping mall. This portion is also modeled with fixities around the first five floors to see the limit behavior of the building. The real behavior of the building will be between two limits such that fully fixed or fully free.

In order to have a realistic mathematical model, different modeling techniques are used such that core walls are modeled with shell elements and frame elements in two different models and these two models are compared for the possible behavior differences. Modeling the shear walls as frame elements is questionable from the point of view that for those large cross-sections compared to their lengths, frame elements may not be working realistically. However it is found out that, frame-element model and shell-element model do not show significant differences based on modal frequency and mode shape comparison shown in Table 4.1.

Table 4.1. Modal frequency comparison of fixed constraint model and stick model

| $E_{cj}$ = 33234 MPa | Non-Updated Frequencies (Hz) | | | | | |
|---|---|---|---|---|---|---|
| | Mode No | Frame Model | | Shell Model | | Identification Results |
| | | Fixed | Stick | Fixed | Stick | |
| X dir. | 1 | 0.8 | 0.54 | 0.84 | 0.56 | 0.61 |
| | 2 | 3.95 | 2.63 | 4.12 | 2.77 | 2.19 |
| | 3 | 8.73 | 6.22 | 9.25 | 6.62 | 5.01 |
| | 4 | 13.7 | 10.09 | 14.7 | 10.89 | 6.59 |
| Y dir. | 1 | 0.75 | 0.51 | 0.75 | 0.52 | 0.61 |
| | 2 | 3.36 | 2.3 | 3.28 | 2.27 | 2.19 |
| | 3 | 7.17 | 5.12 | 6.99 | 5.02 | 5.25 |
| | 4 | 11.5 | 8.3 | 11.4 | 8.19 | 6.59 |

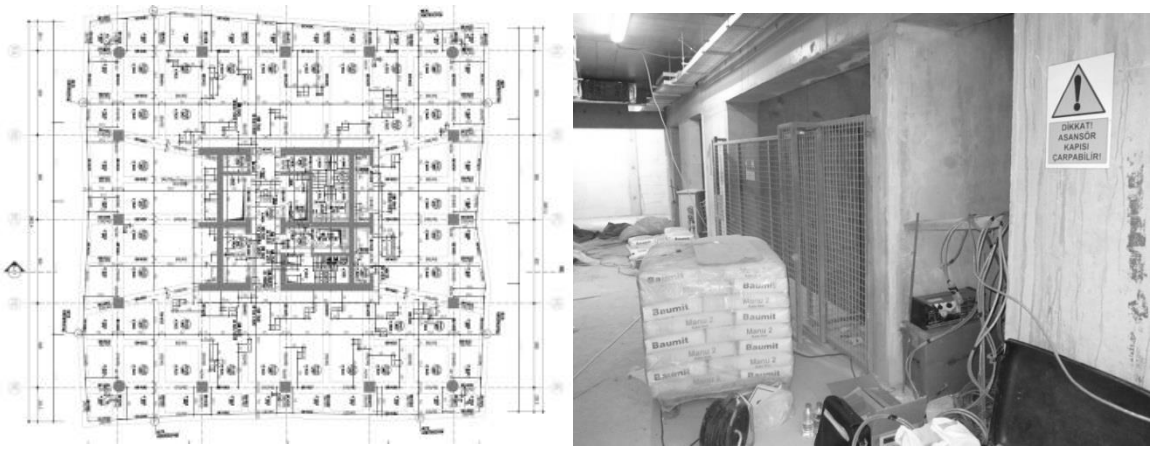


Figure 4.2. The view of shear wall core in the architectural drawings and its photo.

Therefore, shell-element-core model, as shown in Figure 4.2 and Figure 4.3, is chosen to continue the analyses phase.

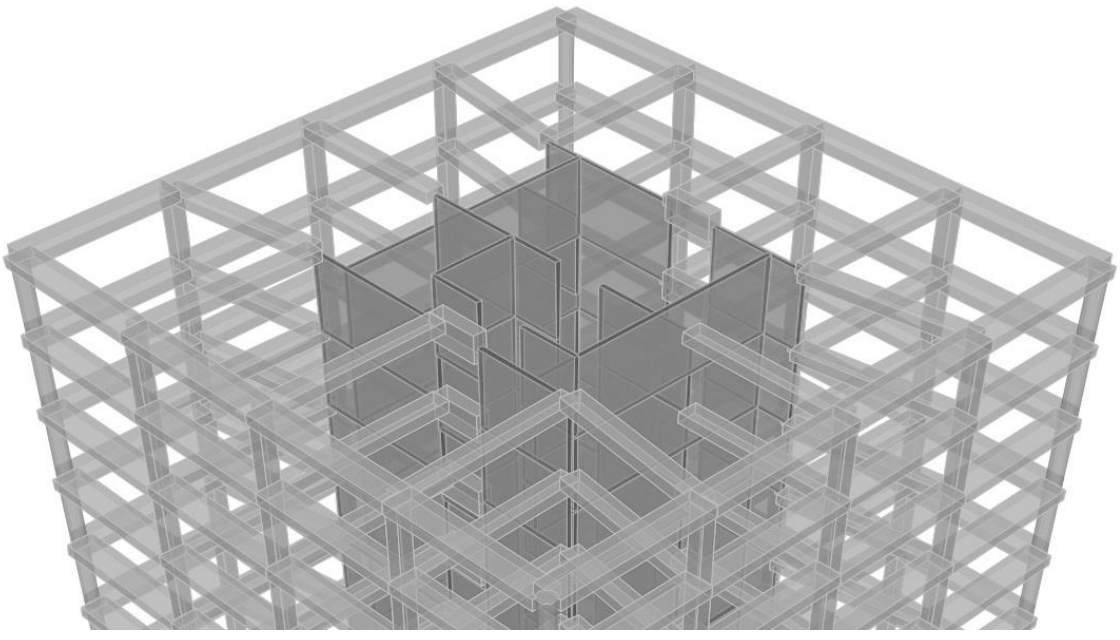

Figure 4.3. Zoomed view of the core walls.

The foundation of the building is not modeled and assumed as fixed for the sake of simplicity for both cases. Moreover, the tower itself has a very irregular plan which is overcome by simplifying the model in terms of frames. In each floor there are 16 columns whose dimensions are changing in different floors. Beams are also changing in dimension

in different floors and 28 main beams for each floor are modeled. Building has a shear wall core in the middle. This core is modeled with detail, openings and internal walls are included in the model. All the frame and wall elements are modeled as massless elements. In order to assign the mass to the system, in each floor, all column, beam, wall and slab masses are calculated and assigned as 1100 tons point mass in story center of mass. Moreover a rigid diaphragm is assigned for the all points in each floor in order to mimic the effect of slab which moves as a whole body in reality. In all column-beam connections, rigid end zones are assigned. For shear walls, thin-shell elements are used. In order not to have cumbersome calculations, mesh numbers are kept low as 4 to 6 for each shell element according to their sizes. Effects of the mesh numbers are investigated. In this investigation several mesh numbers are tested up to 1000 and it is seen that there is a convergence of frequency with increasing mesh number. However, large mesh numbers are introducing cumbersome calculations. These numbers are found out to be performing well for the desired analyses when the operation time and the results are evaluated.

Modulus of elasticity for concrete is described in several design codes by different formulas. The American Concrete Institute (ACI) Code (2008), Eurocode 2 (2005) and Turkish Standards (TS-500) provides the Equation 3.1, Equation 3.2, Equation 3.3 respectively such as

$$E_{cj} = 4700.\sqrt{f_{cj}} \tag{3.1}$$

$$E_{cj} = 9500.\left(f_{cj} + 8\right)^{1/3} \tag{3.2}$$

$$E_{cj} = 3250.\sqrt{f_{cj}} + 14000 \tag{3.3}$$

where $E_{cj}$ is the modulus of elasticity, $f_{cj}$ is the compressive strength.

As the concrete class used in this building is 50 MPa, initial elastic modulus of concrete for C50 is calculated as 33263 MPa, 36773 MPa, 36981 MPa according to

Equation 3.1, Equation 3.2 and Equation 3.3, respectively. The natural frequencies of the non-updated model for these values of modulus of elasticity are shown Table 4.2. For cracked section inertias 0.7 is used as a constant from ACI Code (2008). Therefore all the modulus of elasticity of concrete values are multiplied with 0.7.

Table 4.2. The effect of different modulus of elasticity of concrete values on the natural frequencies of model.

| Natural Frequencies (Hz) | | | | | | |
|---|---|---|---|---|---|---|
| Mode no | Modulus of Elasticity of Concrete | | | | | |
| | $E_{cj}$ = 23263 MPa | | $E_{cj}$ = 25741 MPa | | $E_{cj}$ = 25887 MPa | |
| | X-direction | Y-direction | X-direction | Y-direction | X-direction | Y-direction |
| 1st | 0.47 | 0.43 | 0.49 | 0.46 | 0.49 | 0.46 |
| 2nd | 2.32 | 1.9 | 2.44 | 2 | 2.44 | 2.01 |
| 3rd | 5.54 | 4.2 | 5.82 | 4.41 | 5.84 | 4.43 |
| 4th | 9.11 | 6.85 | 9.58 | 7.21 | 9.61 | 7.23 |

In structural dynamics, damping has a significant role on the response of the structure. In this study damping ratio is set as 5% and 2% for different models. The effect of damping ratio as a structural parameter and Rayleigh Damping is shown in Equation 3.4, Equation 3.5 and Equation 3.6.

$$C = \alpha . M + \beta . K \tag{3.4}$$

where C is the damping matrix, M is the mass matrix, K is the stiffness matrix.

The coefficients, α and β, involve damping ratio parameter such as

$$\alpha = \xi . \frac{2 . \omega_i . \omega_j}{\omega_i + \omega_j} \tag{3.5}$$

$$\beta = \xi . \frac{2}{\omega_i + \omega_j} \tag{3.6}$$

where $\omega_i$ is the ith modal frequency, $\omega_j$ is the jth modal frequency, $\xi$ is the damping ratio.

Modal parameters obtained from the non-updated model with those initial values are shown in Table 4.3, Figure 4.4 and Figure 4.5.

Table 4.3. Frequencies of non-updated model with stick model of restraining effect and shell-elements in the core wall.

| **Mode No** | **FEM Natural Frequencies (Hz)** | |
|---|---|---|
| | **X direction** | **Y direction** |
| **1st** | 0.47 | 0.43 |
| **2nd** | 2.31 | 1.9 |
| **3rd** | 5.53 | 4.19 |
| **4th** | 9.11 | 6.85 |

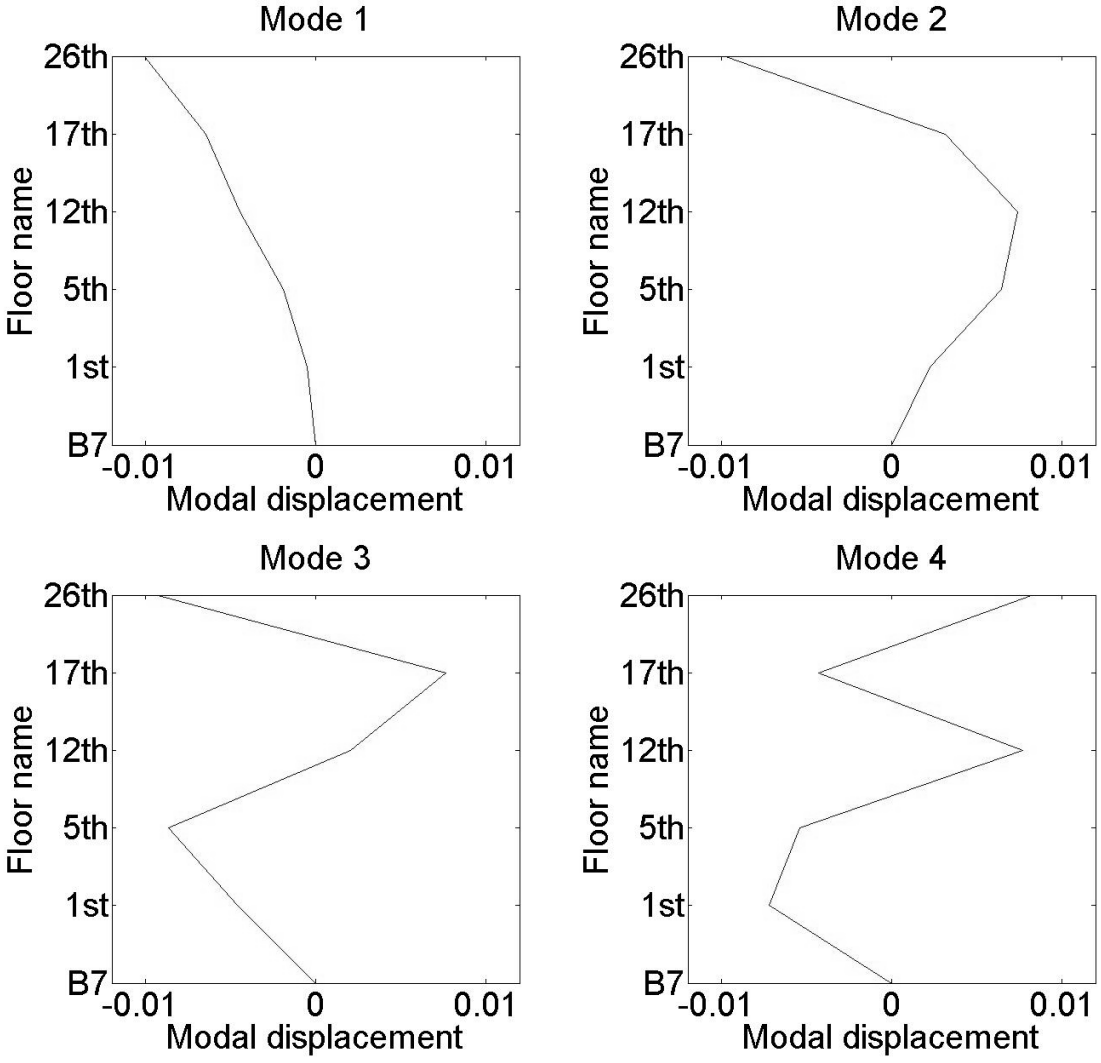


Figure 4.4. Mode shapes of the mathematical model in X direction.

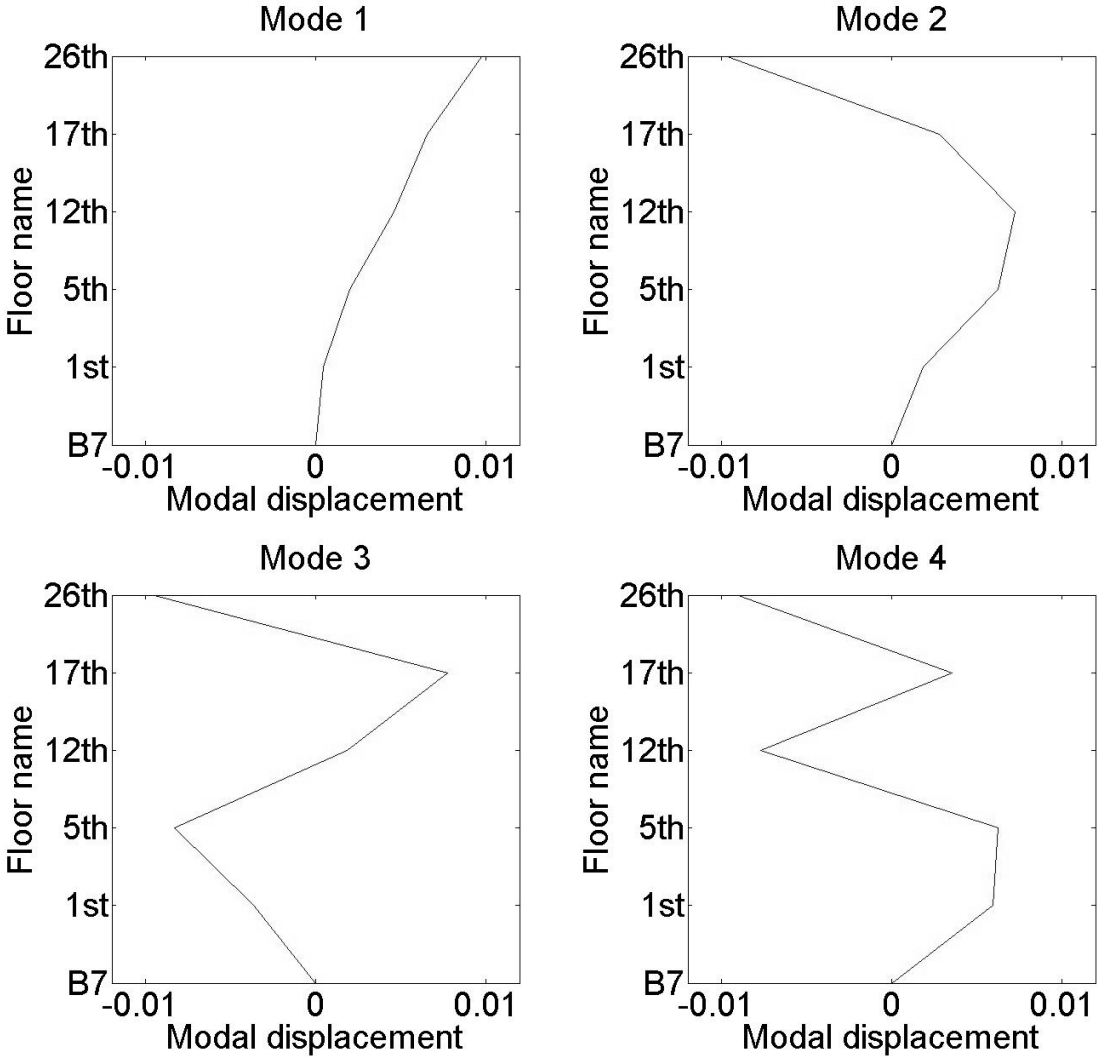


Figure 4.5. Mode shapes of the mathematical model in Y direction.

In the process of modeling, it is significantly seen that modeling uncertainties and the assumptions which are made have a very strong influence on the analyses results. For example the effects of the shopping mall around the tower and the effects of the underground part of the tower directly change the dynamic behavior of the analytical model. Similar behavior can be seen as a result of selected modeling technique, such as using stick elements or shell elements in modeling shear walls. Even meshing density used in shell elements has a big influence on dynamic characters of the model. Moreover, uncertainties that cannot be modeled from architectural drawings such as the weight introduced as a result of non-structural components in the building change the dynamic properties of the building. Another assumed structural parameter, namely damping ratio of the building, is investigated as a comparison of widely used value of 5% for reinforced

concrete buildings and a more realistic value 2% for such a tall building. It showed us that damping ratio assumption has a significant role on the response of the building which will be explained in the following chapters.

In conclusion, just like uncertainties in the stiffness properties of the elements due to uncertainties in material properties or detailing; weights from non-structural components in the building and more significantly modeling techniques used such as stick elements or shell elements for shear walls or even mesh rate for the shell elements affect the outcomes.

# 5. FEM UPDATING

## 5.1. Error Function

For each model with a different combination of modal parameters, a modal analysis is run, following that modal shapes and natural frequencies are obtained as modal parameters from these analyses. These modal shapes and natural frequencies are used in finite element model updating as parameters in the error function to be optimized. In this error function, measured modal parameters which are obtained via FDD from acceleration data is included and used as target values. In addition to that, confidence levels are also included in error function in terms of multiplication of weighing constants. These errors are in percentage such that difference between measured modal parameters and obtained modal parameters from the mathematical models divided by measured modal parameters. Square values of those are taken in order to get errors in positive values. This error calculation includes both natural frequencies and modal shapes as modal parameters. This error values are calculated via modal assurance criteria (MAC) as shown in Equation 5.1.

$$MAC = \frac{|\psi_*^T . \psi|^2}{(\psi_*^T . \psi_*).(\psi^T . \psi)} \tag{5.1}$$

where $\psi_*$ is the measured mode shape, $\psi$ is the simulated mode shape of corresponding mode.

In terms of MAC, the value 1 shows the exact match. Therefore, the error value is obtained by subtracting the MAC value from 1.

The weighing constants are defined according to the modal participation factors of corresponding modes. As the first mode has a more dominant effect on vibration characteristics, this approach favors first mode, second mode and the third mode in a decreasing fashion respectively. Error function is described as Equation 5.2.

$$E(\alpha_1, \alpha_2, \alpha_3, \beta_1, \beta_2, \beta_3) = \sum_{i=1}^{3} (k_i . [(f_i^* - f_i)/f_i^*]^2 + h_i . [1 - MAC_i]^2) \qquad (5.2)$$

where $\alpha_1, \alpha_2, \alpha_3$ are first, second and third natural frequencies respectively while $\beta_1, \beta_2, \beta_3$ are first, second and third mode shapes respectively. $k_i$ and $h_i$ values are assigned as 0.8, 0.15 and 0.05 for first, second and third step respectively, as it is described above corresponding the modal participation factors.

The Matlab code used reads the created output files and takes the first four natural frequencies and mode shapes. The code compares these values with the initially given identified natural frequencies and mode shapes for 1000 different combinations. Then the code calculates the error according to the Equation 5.1 and Equation 5.2. Finally, code selects the combination with minimum error.

As described above, modal parameters are updated using 1000 different combinations of updating parameters. Updated and non-updated natural frequencies and mode shapes are shown in Table 5.1.

Table 5.1. Frequency Comparison

| **Mode No** | **System Identification Frequencies (Hz)** | **Non-updated FEM Frequencies (Hz)** | **Updated FEM Frequencies (Hz)** |
|---|---|---|---|
| **1st** | 0.61 | 0.43 | 0.60 |
| **2nd** | 2.19 | 1.90 | 2.65 |
| **3rd** | 5.25 | 4.19 | 5.85 |
| **4th** | 6.59 | 6.85 | 9.56 |

As shown in Table 5.1, non-updated FEM frequencies are lower than system identification frequencies except for the fourth mode. As a result of increase in modulus of elasticity of concrete in order to match the higher system identification frequencies, namely the first, the second and the third modes, natural frequency of the fourth mode is also increasing in as it is supposed to decrease. As the reason for difference between

natural frequencies of high modes of system identification results and mathematical model cannot be fully clarified, fourth mode natural frequency and mode shape are not used in system identification process. Moreover, it should be noted that as modal participation factors of first three modes are in a decreasing order, the importance of the accuracy of these modes are also decreasing. In other words, as first mode has the highest modal participation factor, it has the biggest influence on the dynamic performance of the building. Therefore, a higher accuracy in this mode will lead to a better accuracy in the performance of the building as well.

It should be noted that, in literature it is theoretically and experimentally shown that there is a ratio between the natural frequencies of the buildings. Li and Mau (1997) showed that for the theoretical case, in the perfect shear deformation case, the ratio between 1st and 2nd modes is 3; the ratio between 1st and 3rd modes is 5. In the perfect bending case the ratio between 1st and 2nd modes is 6.3, the ratio between 1st and 3rd modes is 17.5. For the experimental case, for the frame dominated buildings the ratio between 1st and 2nd modes is 3; the ratio between 1st and 3rd modes is varying between 4 and 6. For the shear-wall dominated buildings the ratio between 1st and 2nd modes is varying between 3 and 5; the ratio between 1st and 3rd modes is varying around 8. Therefore, the results of this study showed that the building is behaving in a bending or in another words shear-wall dominated fashion. In the identified natural frequencies, these ratios are quite close to the findings above. On the other hand, the ratios between the natural frequencies of the FEM seem to be more than that.

In conclusion, it is observed that, system identification and finite element updating significantly decreased the error between measured modal parameters and those obtained from mathematical models, therefore resulted in much more realistic models for damage estimation.

### 5.2. Matlab Code and Model Generation / Matlab – SAP2000 Integration

In Figure 5.1, a representative scheme can be seen for the Matlab - SAP2000 integration.

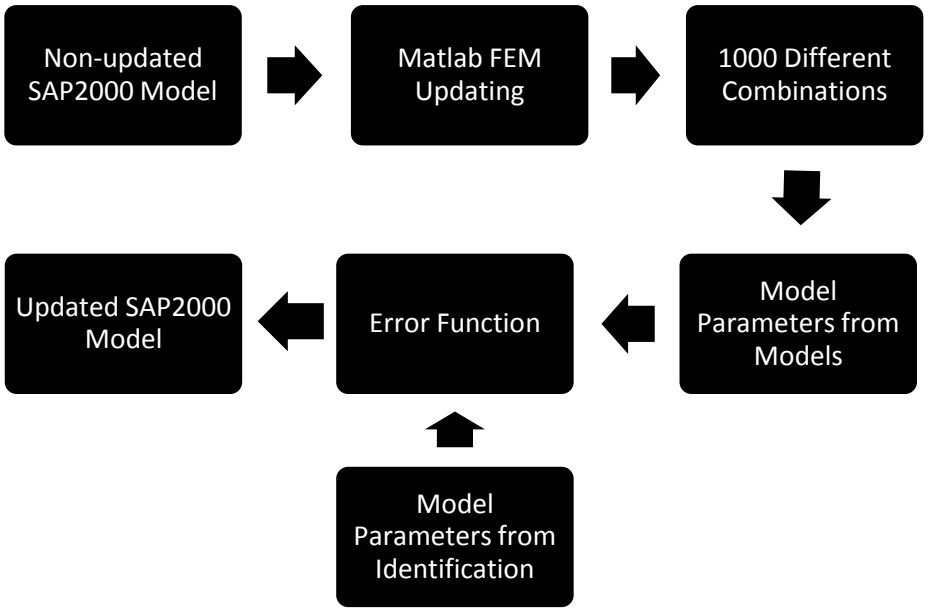


Figure 5.1. FEM Updating Flowchart.

Generally there are lots of assumptions made in design/modeling of structures in any engineering field. This is a natural result of the difficulties in trying to mimic the real or physical world. Thus, understanding the realistic dynamic behavior of the building, FEM Updating has very important role. As a result of this need, FEM updating is applied to see the response of the updated building model under several possible earthquake scenarios. With FEM Updating process, mathematical model of the building will be behaving as close as possible to the real building. For example, mathematical model which is created on several assumptions may stay on the safe side on a given earthquake simulation while an updated thus a much more realistic mathematical model may become unsafe as a result of earthquake loads applied on the building.

FEM updating is carried out via Matlab platform. An iterative program is written to automatically update desired structural parameter. In model updating three parameters are

used: Modulus of elasticity of the concrete, dimensions of the stick element in the x and y direction.

First, the non-updated model of the building is created as described in Chapter 4. This model is used in FEM updating process as an initial point. In FEM updating code, this initial point is set as a text file, which includes all the information of the building. This text file is created according to the information in the .$2k file of the model in SAP2000 folder. This input file is used in order to import the desired model in SAP2000 software which is run by Matlab program. This automatic process let the user only enter the input once rather then, running hundreds or thousands of simulations with different settings in each one.

Once this file is set as an input, the FEM updating code can find the initial values of any desired parameters, which are modulus of elasticity of concrete and the X and Y dimensions of the stick model in this case, and change them with the new iteration values. The resolution of the simulations can be changed by increasing or decreasing the step value for the parameters. It is again a decision between accuracy of the simulation and calculation burden on the operation. Afterwards, for each combination outputs are written and saved as an Excel file. Following that, FEM updating code reads the desired output values, which are natural frequencies and join displacements for modal case to calculate mode shapes, and use them in a cost function, which also uses the obtained system identification values in order to calculate the error between experimental and analytical modal parameters. As a result, FEM updating code choses the best combination between 1000 models which behaves closer to the real building.

For the modulus of elasticity one coarse and one finer analysis are run. In these analyses, modulus of concrete is set for ten different values increasing 1000 MPa in each iteration. For the stick model, both in longitudinal and transverse dimensions of the stick are set for ten different values which are increased 1m in each iteration starting from 0.1 m. As a result 1000 different combination is investigated by creating 1000 different models. This is done by a code written in Matlab. Then again via Matlab, desired values which are modal displacements (in order to calculate mode shapes) and natural frequencies are read from output files. Then a cost function is used to calculate the error of each model and

select the combination with the smallest error. In error calculation, first, second and third natural frequencies and the first, second and third mode shapes are used with corresponding weighing constants defined according to the modal participation factors of these modes.

The errors are plotted for each combination simulated in Figure 5.2.

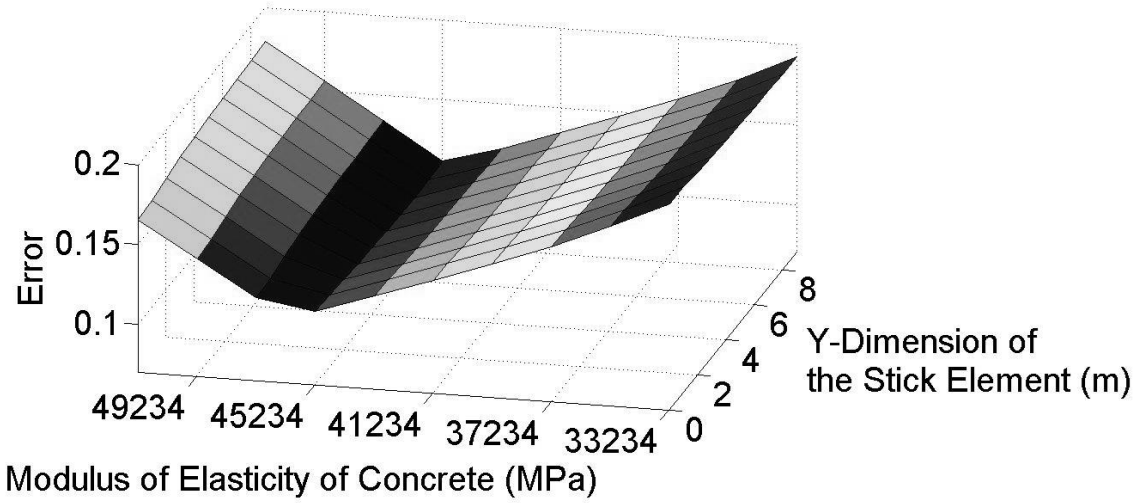


Figure 5.2. Error results of simulated combinations.

In the figure above, error results of 1000 different simulations are demonstrated. Simulations can be divided into ten groups with different modulus of elasticity. Each group has 100 simulations with different stick element dimensions. Therefore it can be seen that error function has a pattern and a minimum value around 11.5%.

# 6. SEISMIC DEMAND

In the seismic demand section of the study, Pacific Earthquake Engineering Research Center (PEER) Tall Buildings Initiative (TBI) Version 1.0 (2010) is followed as a methodology guide. It is an overall study which brings an alternative way to comparing design codes to design and evaluate the performance of the tall buildings. In some cases, TBI is pioneering the high performance structural and earthquake engineering for the tall buildings. Therefore, TBI is used as a guide in order to find the appropriate approaches for the local characteristics such as the site of the building investigated in this study. For example, in order to evaluate the characteristics of North Anatolian Fault the TBI is used as a guide to find the proper analysis methods.

North Anatolian Fault is one of the most important fault lines in Anatolia which is a very active seismic area with several major and lots of minor fault lines crossing across. This fault line is crossing Anatolia from one end to other and produced lots of major earthquakes throughout the history. Lots of historical records show that, very destructive earthquakes are produced by this fault line. The last two of them are devastating Kocaeli (M=7.4) and Duzce (M=7.2) earthquakes which occurred in 1999. Following the East-West route, this fault line dives into Marmara Sea and continue to the West, closing to Istanbul shores nearly 10-20 km. While trying to anticipate the seismic demand of the building this fault line is considered as the main risk source. The building site is in the approximately 20-30 km north of the fault line. Therefore, twenty nine earthquake records are obtained from PEER database to simulate the seismic demand on the building. These ground motion data are selected according to their magnitude, distance and PGA values. These values are selected according to expected earthquake in Istanbul which is approximated as magnitude 7.5, and the fault segment is 20-30 km away to the building site as suggested by Erdik *et al.* (2004). Building site is shown with a star in the map of the Marmara segment of North Anatolian Fault which is taken from the website of Republic of Turkey Prime Ministry Disaster and Emergency Management Presidency and can be seen in Figure 6.1 (www.afad.gov.tr).

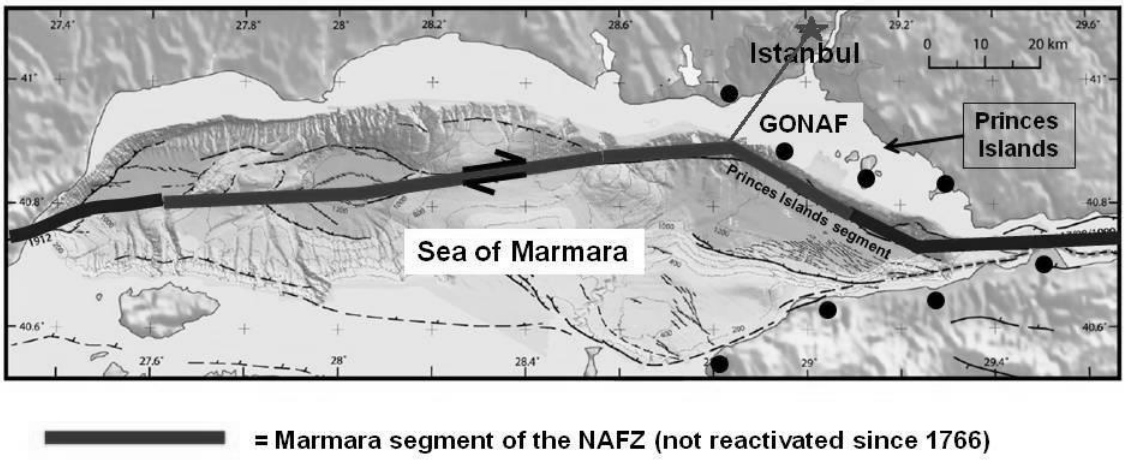


Figure 6.1. Marmara segment of North Anatolian Fault Zone and the location of the building.

Records used as excitation sources, their distance, magnitude and PGA values and obtained interstory drift ratios from the analyses can be seen in Table 6.1.

Table 6.1. Earthquake records

| Earthquake Name | Magnitude | Distance (km) | PGA (g) | Maximum Interstory Drift Ratio (%) | | | |
|---|---|---|---|---|---|---|---|
| | | | | Non-updated | | Updated | |
| | | | | 2% Damping Ratio | 5% Damping Ratio | 2% Damping Ratio | 5% Damping Ratio |
| Cape Mendocino (1) | 7.1 | 18.5 | 0.549 | 0.224 | 0.188 | 0.251 | 0.197 |
| Cape Mendocino (2) | 7.1 | 33.8 | 0.229 | 0.026 | 0.023 | 0.019 | 0.013 |
| Chi-Chi, Taiwan (1) | 7.6 | 26 | 0.639 | 0.27 | 0.193 | 0.158 | 0.117 |
| Chi-Chi, Taiwan (2) | 7.6 | 43.4 | 0.712 | 0.289 | 0.242 | 0.191 | 0.134 |
| Coalinga (1) | 6.4 | 25.5 | 0.281 | 0.195 | 0.157 | 0.119 | 0.099 |

Table 6.1. Earthquake records (Cont.)

| Earthquake Name | Magnitude | Distance (km) | PGA (g) | Maximum Interstory Drift Ratio (%) | | | |
|---|---|---|---|---|---|---|---|
| | | | | Non-updated | | Updated | |
| | | | | 2% Damping Ratio | 5% Damping Ratio | 2% Damping Ratio | 5% Damping Ratio |
| Coalinga (2) | 6.4 | 29.9 | 0.282 | 0.294 | 0.247 | 0.295 | 0.26 |
| Duzce, Turkey | 7.1 | 17.6 | 0.822 | 0.408 | 0.306 | 0.314 | 0.262 |
| Friuli, Italy | 6.5 | 37.7 | 0.351 | 0.18 | 0.13 | 0.121 | 0.103 |
| Imperial Valley (1) | 6.5 | 10.4 | 0.315 | 0.452 | 0.37 | 0.246 | 0.188 |
| Imperial Valley (2) | 6.5 | 43.6 | 0.351 | 0.42 | 0.34 | 0.607 | 0.409 |
| Irpinia, Italy (1) | 6.5 | 32 | 0.358 | 0.842 | 0.597 | 0.264 | 0.243 |
| Irpinia, Italy (2) | 6.5 | 33 | 0.217 | 0.097 | 0.072 | 0.095 | 0.071 |
| Kobe (1) | 6.9 | 15.5 | 0.243 | 0.33 | 0.262 | 0.123 | 0.109 |
| Kobe (2) | 6.9 | 26.4 | 0.345 | 0.297 | 0.266 | 0.557 | 0.369 |
| Kocaeli, Turkey (1) | 7.4 | 17 | 0.244 | 0.189 | 0.181 | 0.165 | 0.132 |
| Kocaeli, Turkey (2) | 7.4 | 78.9 | 0.249 | 0.169 | 0.16 | 0.176 | 0.145 |
| Landers (1) | 7.3 | 21.2 | 0.417 | 0.234 | 0.188 | 0.268 | 0.209 |
| Landers (2) | 7.3 | 24.9 | 0.245 | 0.344 | 0.25 | 0.356 | 0.317 |
| Loma Prieta (1) | 6.9 | 16.9 | 0.638 | 0.162 | 0.148 | 0.212 | 0.169 |
| Loma Prieta (2) | 6.9 | 21.8 | 0.484 | 0.348 | 0.272 | 0.244 | 0.2 |
| Northridge (1) | 6.7 | 20.8 | 0.617 | 0.18 | 0.145 | 0.264 | 0.215 |
| Northridge (2) | 6.7 | 27.6 | 0.883 | 0.607 | 0.487 | 0.362 | 0.274 |

Table 6.1. Earthquake records (Cont.)

| Earthquake Name | Magnitude | Distance (km) | PGA (g) | Maximum Interstory Drift Ratio (%) | | | |
|---|---|---|---|---|---|---|---|
| | | | | Non-updated | | Updated | |
| | | | | 2% Damping Ratio | 5% Damping Ratio | 2% Damping Ratio | 5% Damping Ratio |
| San Fernando (1) | 6.6 | 20.3 | 0.366 | 0.058 | 0.043 | 0.064 | 0.051 |
| San Fernando (2) | 6.6 | 24.9 | 0.324 | 0.107 | 0.07 | 0.07 | 0.062 |
| Superstitn Hills (1) | 6.7 | 24.4 | 0.408 | 0.048 | 0.035 | 0.032 | 0.024 |
| Superstitn Hills (2) | 6.7 | 28.3 | 0.247 | 0.197 | 0.162 | 0.134 | 0.095 |
| Tabas, Iran | 7.4 | 17 | 0.406 | 0.267 | 0.219 | 0.215 | 0.174 |
| Taiwan SMART1 (1) | 6.4 | 64 | 0.254 | 0.152 | 0.134 | 0.157 | 0.142 |
| Taiwan SMART1 (2) | 7.3 | 39 | 0.242 | 0.275 | 0.191 | 0.165 | 0.121 |

Two maximum interstory drift ratios are set as 2% and 5%. These values are determined according to the economic value of building complex as the damage in an expected earthquake should be at minimum. For the non-updated and 2% damping ratio scenario, there are 16 earthquake records above the 2% maximum interstory drift ratio limit out of 29 records. In the case of the 5% maximum interstory drift ratio limit, there are 2 earthquake records above the limit out of 29 records. After updating process for the same damping ratio, there are 12 earthquake records above the 2% maximum interstory drift ratio limit out of 29 records and 2 earthquake records above the 5% maximum interstory drift ratio limit out of 29 records. Due to the frequency change caused by FEM updating, maximum interstory drifts are changing according to frequency content of earthquake record used.

On the other hand, for the non-updated and 5% damping ratio scenario, there are 12 earthquake records above the 2% maximum interstory drift ratio limit out of 29 records. In the case of the 5% maximum interstory drift ratio limit, there are 1 earthquake records

above the limit out of 29 records. After updating process for the same damping ratio, there are 10 earthquake records above the 2% maximum interstory drift ratio limit out of 29 records and no earthquake records above the 5% maximum interstory drift ratio limit out of 29 records.

Response spectra of selected ground motions, their mean, the design spectrum in the Turkish Earthquake Code (2007) and two other alternative design spectra are shown in Figure 6.2.

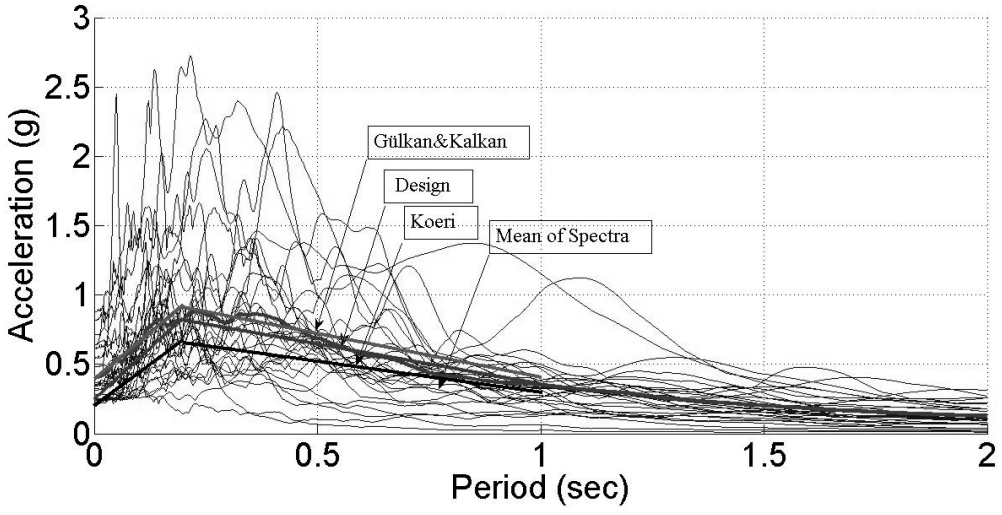


Figure 6.2. Response spectra and several design codes.

As it can be seen in the response spectra graph, response spectrum of the building will be directly correlated with the selection of the earthquake records. Therefore, earthquake selection becomes an important issue in seismic assessment of the structures. Especially in tall buildings, like the one investigated in this research, natural vibration periods of the buildings will be definitely longer than ordinary buildings. As the period of the buildings increasing, corresponding longer period acceleration values will be defining the dynamic behavior of the building. Therefore, selecting earthquake records with high acceleration values corresponding to the natural frequencies of the building must be considered.

Another important point is the selection of a proper design code/design spectrum as the selected earthquake records will be evaluated according to the selected design spectrum. Thus, the validity of the selection of earthquake records will be based on the selection of different design spectra. At this point, it should be noted that there is no perfect design spectrum and selection of it must be made according to the specific site and building conditions. Also, the trade-off between safety and economics will be decided according to the selected design spectrum. A higher mean of selected earthquake records will be forced by higher design spectrum and this will result in higher seismic demand on the building. On the other hand, a lower design spectrum will be resulted in a lower mean of selected earthquake records, therefore a lower seismic demand on the building.

It can also be seen in Figure 6.2 that selection of earthquake records are proper as the mean of selection show good compatibility with three design spectra.

A total of 116 time history analyses are run for each updated and non-updated finite element models with 5% and 2% damping ratios for each case. In these analyses earthquake loads are applied in only Y direction. However, in order to be sure about the effects of the earthquakes, three earthquake records, namely Duzce, Kocaeli1 and Northridge2, selected and applied in both directions as earthquake loads for a damping ratio of 5%. As a result it is found out that, difference is only around 0.005% as shown in Figure 6.3, Figure 6.4, Figure 6.5 and Table 6.2.

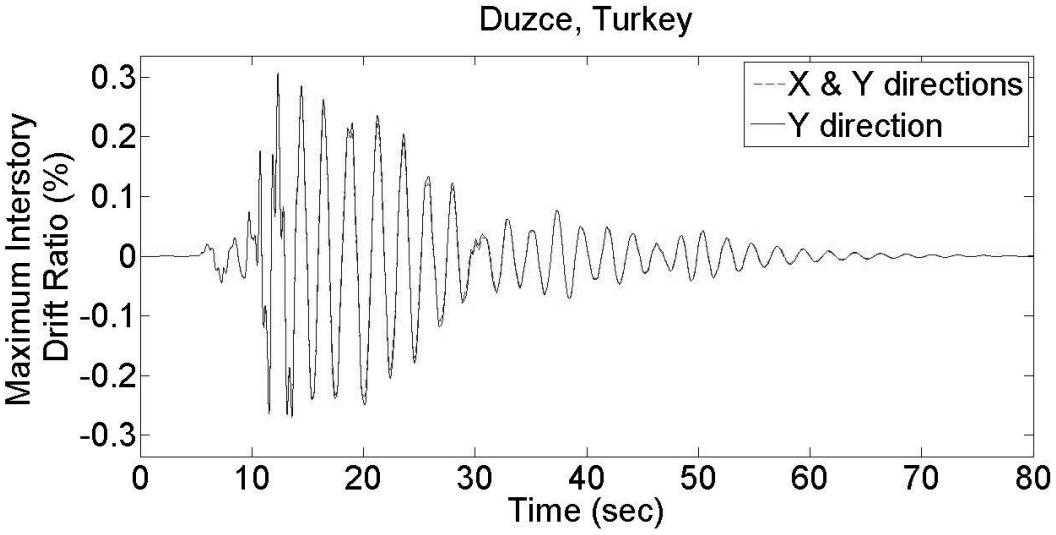


Figure 6.3. 2-directions interstory drift ratio time-history for Duzce, Turkey earthquake record.

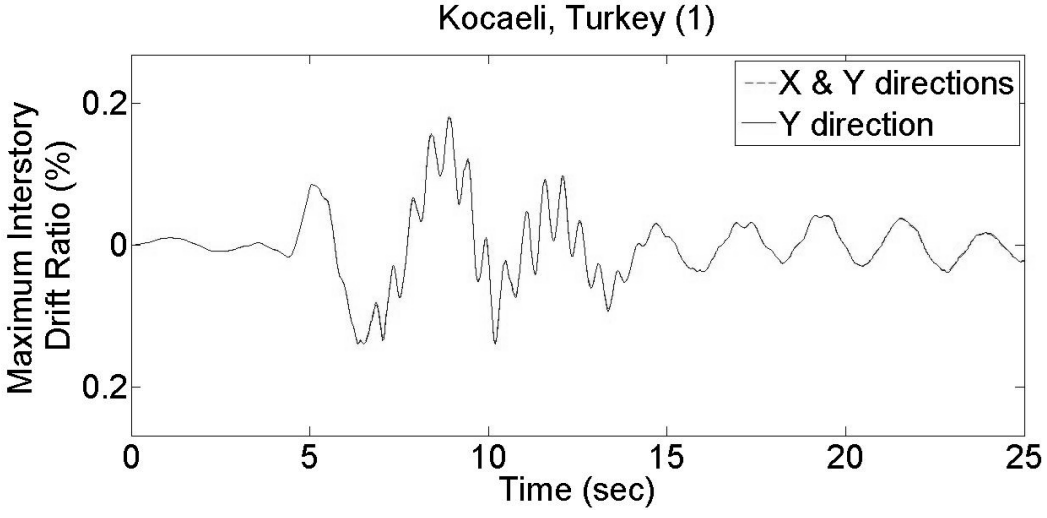


Figure 6.4. 2-directions interstory drift ratio time-history for Kocaeli, Turkey (1) earthquake record.

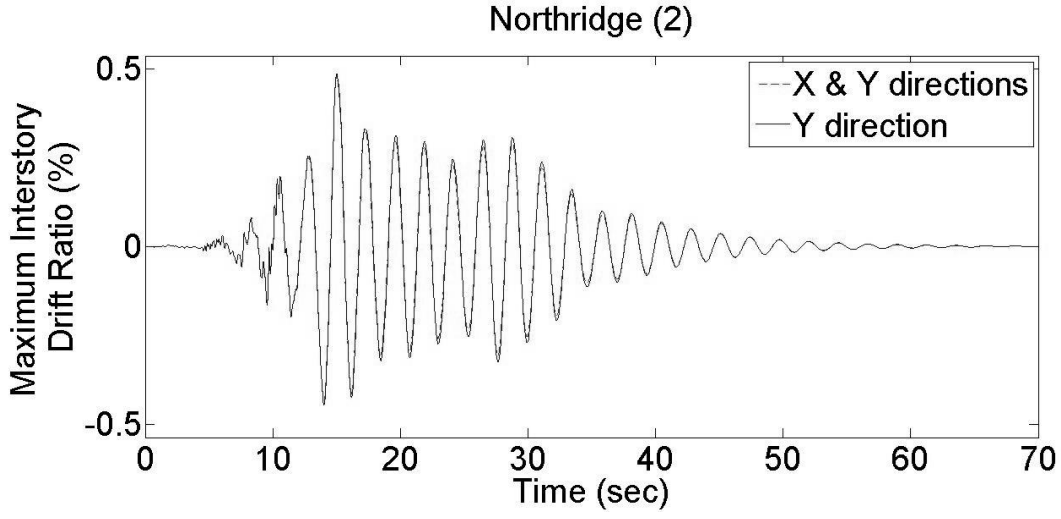


Figure 6.5. 2-directions interstory drift ratio time-history for Northridge (2) earthquake record.

Table 6.2. Maximum Interstory Drift Ratios

| Earthquake name | Non-updated | | Updated | |
|---|---|---|---|---|
| | Y direction (%) | X & Y directions (%) | Y direction (%) | X & Y directions (%) |
| Duzce | 0.306 | 0.303 | 0.262 | 0.259 |
| Kocaeli, Turkey (1) | 0.18 | 0.181 | 0.132 | 0.128 |
| Northridge (2) | 0.487 | 0.482 | 0.274 | 0.271 |

The maximum inter-story drift ratio values show us the effect of updating process. For 2% damping ratio, the biggest increase in maximum interstory drift ratios between the non-updated and updated cases are in the records of Kobe (2), Northridge (1), Imperial Valley (2) and Loma Prieta (1). Increase percentages are 87.5%, 46.7%, 44.5% and 30.9% respectively. Therefore, these selected maximum interstory drift ratio time-histories for the 2% damping ratio are shown in Figure 6.6, Figure 6.7, Figure 6.8 and Figure 6.9 respectively.

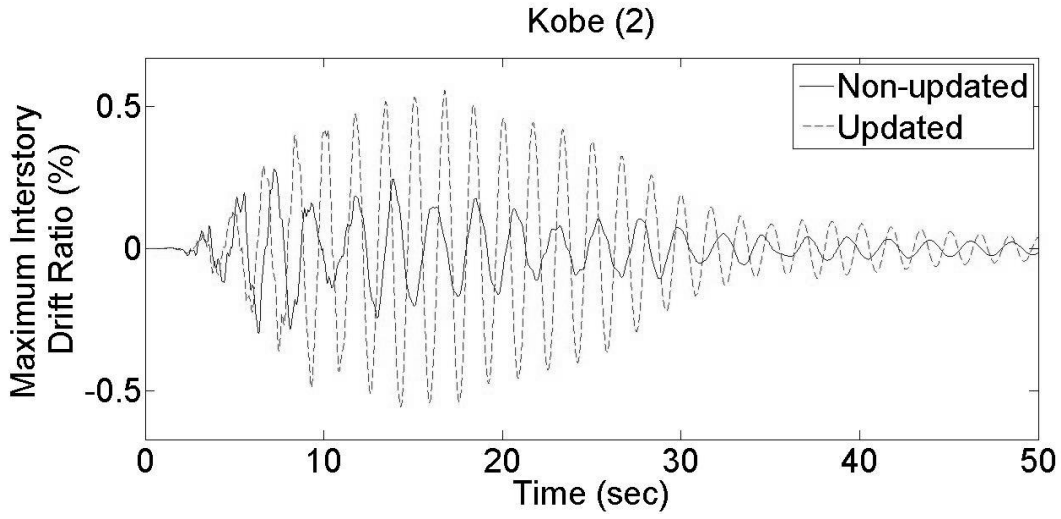


Figure 6.6. Maximum interstory drift ratio time-history of Kobe (2) record for 2% damping ratio.

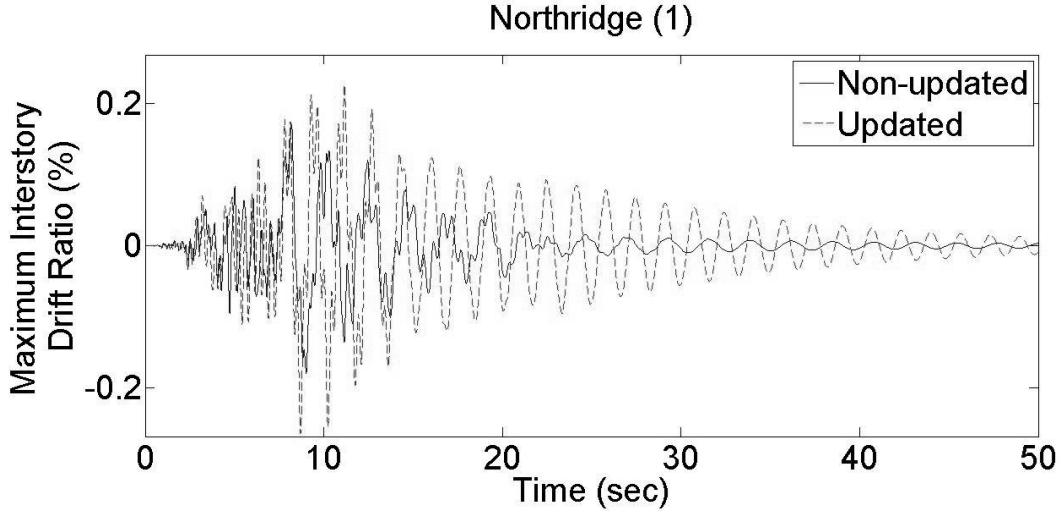


Figure 6.7. Maximum interstory drift ratio time-history of Northridge (1) record for 2% damping ratio.

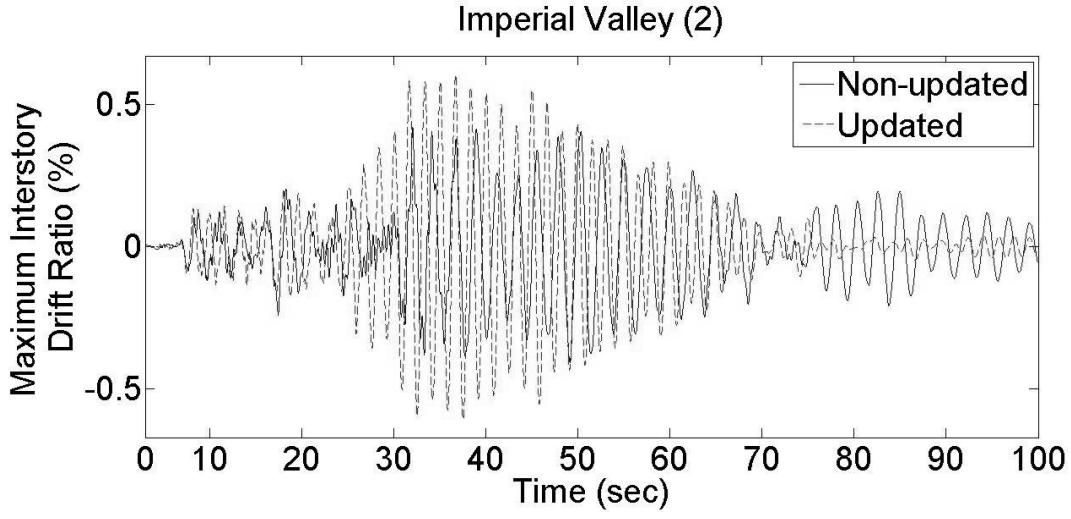


Figure 6.8. Maximum interstory drift ratio time-history of Imperial Valley (2) record for 2% damping ratio.

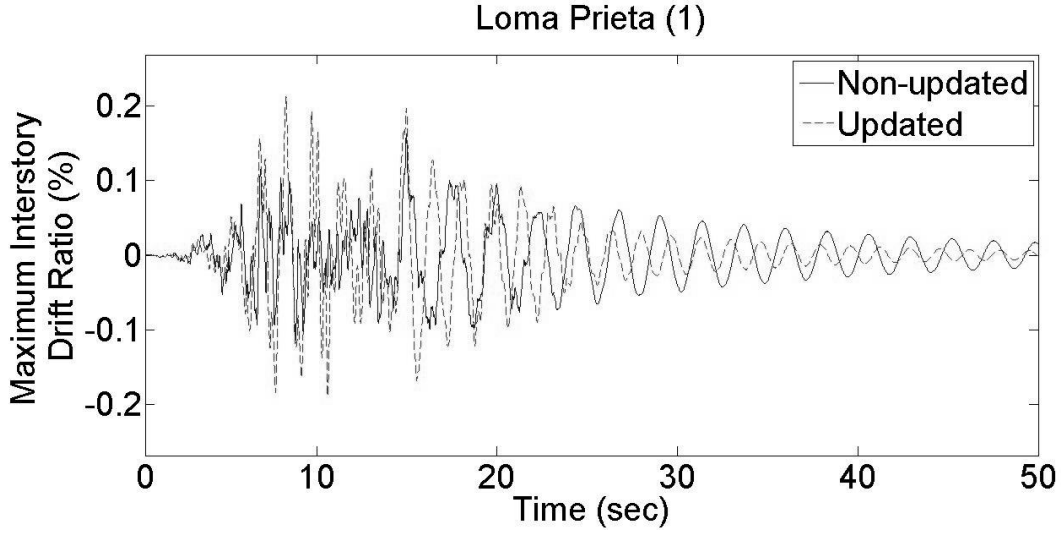


Figure 6.9. Maximum interstory drift ratio time-history of Loma Prieta (1) record for 2% damping ratio.

For 5% damping ratio, the biggest increase in maximum interstory drift ratios between the non-updated and updated cases are in the records of Northridge (1), Kobe (2), Landers (2) and Imperial Valley (2). Increase percentages are 48.3%, 38.7%, 26.8% and 20.3% respectively. Selected maximum interstory drift ratio time-histories for the 5% damping ratio are shown in Figure 6.10, Figure 6.11, Figure 6.12 and Figure 6.13, respectively.

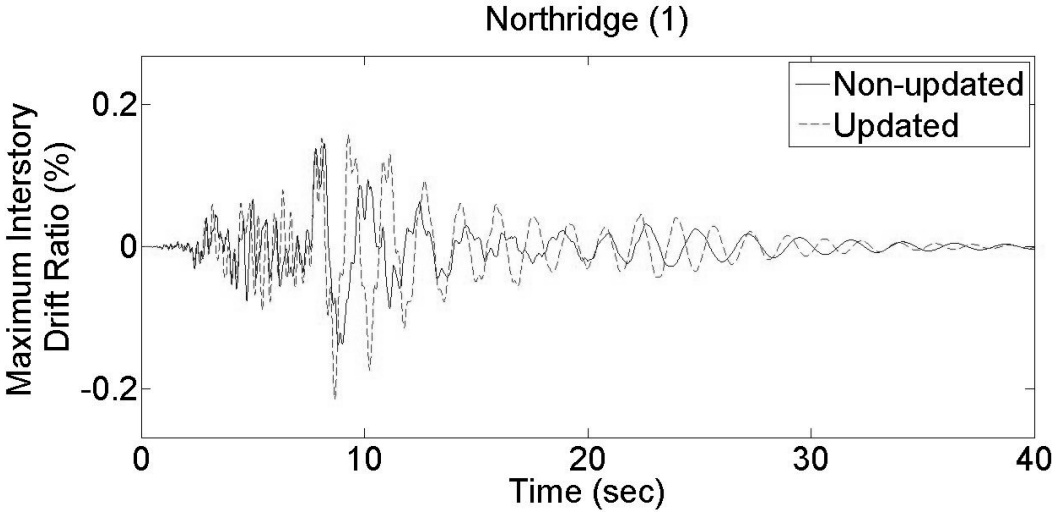


Figure 6.10. Maximum interstory drift ratio time-history of Northridge (1) record for 5% damping ratio.

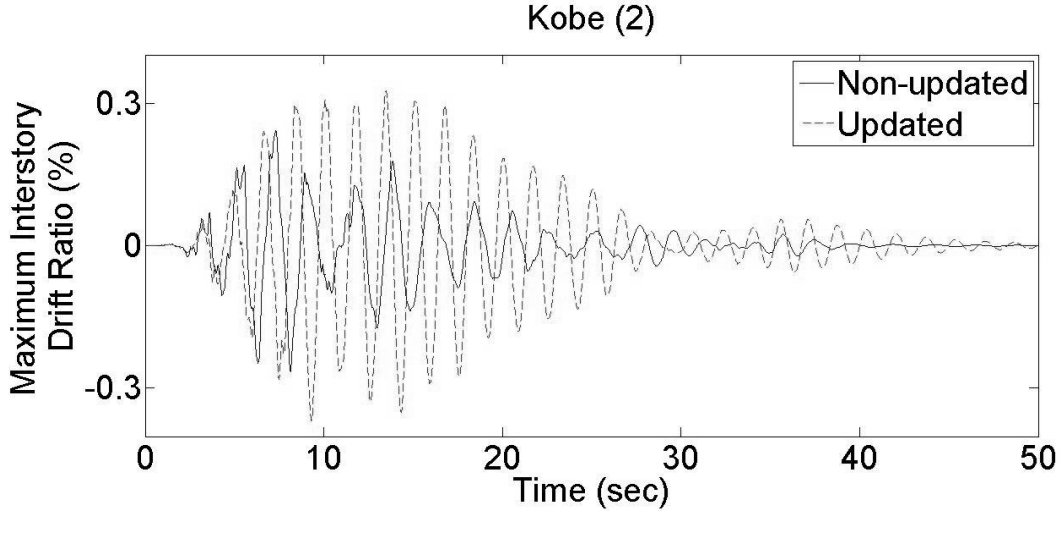


Figure 6.11. Maximum interstory drift ratio time-history of Kobe (2) record for 5% damping ratio.

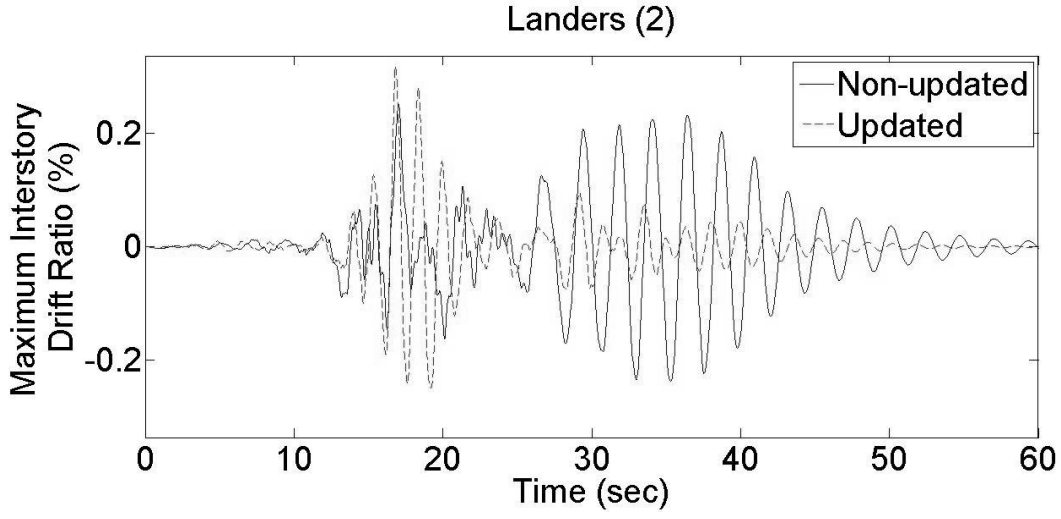


Figure 6.12. Maximum interstory drift ratio time-history of Landers (2) record for 5% damping ratio.

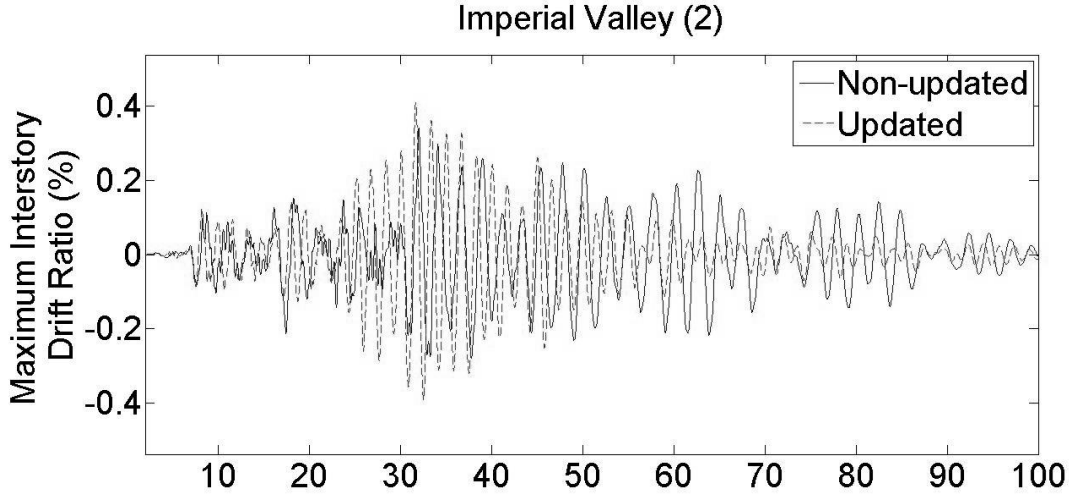


Figure 6.13. Maximum interstory drift ratio time-history of Imperial Valley (2) record for 5% damping ratio.

On the other hand, differences caused by damping ratios are non-ignorable. Interstory drift ratios are compared as a measure for the seismic response of the models. Limits for interstory drift ratios are set according to the economic value of the building as the damage level in an expected earthquake should be at minimum.

Probability density functions of drift ratios for updated and non-updated cases are obtained as shown in Figure 6.14.

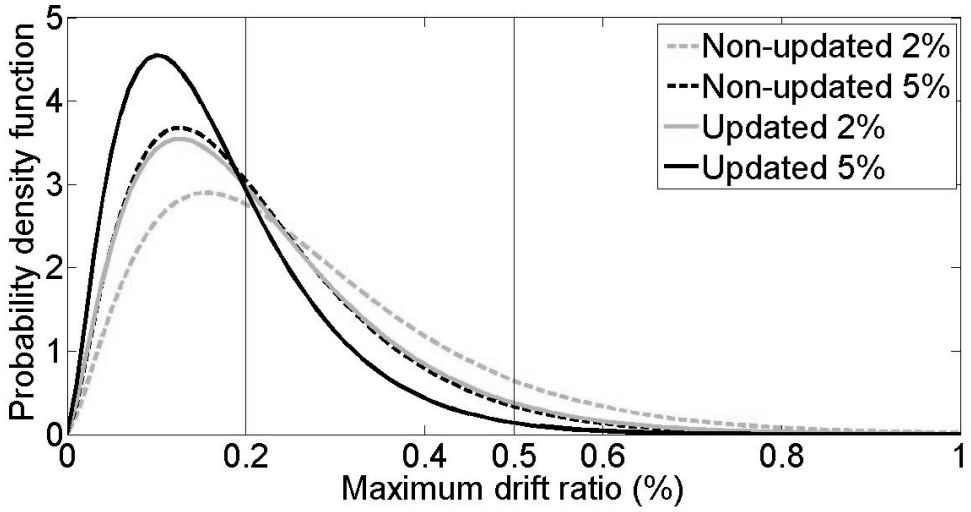


Figure 6.14. Probability density function of updated and non-updated maximum cases for drift ratio values.

Table 6.3. Results of Probability of Failure Analyses

| Probability of Failures | 2% damping | | 5% damping | |
|---|---|---|---|---|
| | Updated | Non-updated | Updated | Non-updated |
| 2% limit | 0.4582 | 0.5776 | 0.3148 | 0.4445 |
| 5% limit | 0.0429 | 0.0938 | 0.0116 | 0.0357 |

In Figure 6.14 and Table 6.3, it can be seen that in case limit drift ratio is set equal to 0.2%, the failure probabilities of updated and non-updated models for 2% damping ratio are 0.4582 and 0.5776, respectively. The same results for the 5% damping ratio are 0.3148 and 0.4445 for updated and non-updated models, respectively. Another example, in order to inspect the behavior around the tail region of the density functions, is that when the limit drift ratio is 0.5%, the failure probabilities of updated and non-updated models for 2% damping ratio are 0.0429 and 0.0938, respectively. The same results for the 5% damping ratio are 0.0116 and 0.0357 for updated and non-updated models, respectively.

For instance, in case of 2% damping ratio, Loma Prieta (1) and Northridge (1) earthquake excitations are expected to cause maximum interstory drift ratios below the 2% limit in non-updated case on the other hand in updated case, these excitations are expected to cause maximum interstory drift ratios above the 2% limit.

The same can be observed in the case of 5% damping ratio, as Landers (1) and Northridge (1) earthquake excitations are expected to cause maximum interstory drift ratios below the 2% limit in non-updated case while in updated case, these excitations are expected to cause maximum interstory drift ratios above the 2% limit.

Another example can be seen in the 5% limit of maximum interstory drift ratio. In the case of 2% damping ratio, Imperial Valley (2) and Kobe (2) earthquake records are expected to cause maximum interstory drift ratios below the 5% limit in non-updated case on the other hand, in updated case these excitations are expected to cause maximum interstory drift ratios above the 5% limit. It should be noted that, for the case of 5% damping ratio, maximum interstory drift ratios are all below the 5% limit for the updated case.

Similarly, the probability distributions of updated and non-updated models show that consideration of vibration measurements, in other words, use of finite element model updating, have a significant effect on structural reliability.

# 7. CONCLUSIONS AND RECOMMENDATIONS

This study covers instrumentation, data acquisition, system identification, finite element modeling and FEM updating of a tall building structure. Moreover, the effect of the proposed procedure on seismic demand is investigated by comparing interstory drift ratios with the non-updated model. Finally, probability density functions of interstory drift ratios are calculated. The study uses the FDD method for system identification. Moreover, FEM updating is carried out considering modulus of elasticity, the dimensions of a stick element, which represent the uncertainties of material, and the boundary conditions due to the shopping mall structure.

The installment of the data acquisition system is a very important step of this study as it is the starting point and affects the rest of the study. The selection of the type of sensors, receiver and the location of sensors are very important by means of collecting healthy data which will establish the base for the following steps. For instance, the selection of sensor location has a direct effect on acquiring the mode shapes of the structure which has an important contribution on the rest of the study.

In the system identification process, it is obvious that, the method applied has a significant effect on the results. Therefore, the selection of the method and the application of this method are very important in order to obtain desired outcomes. In this study, FDD is applied and the natural frequencies are obtained with great care. Mode shapes of these frequencies are used to check in order to be sure about the selection of the frequencies. However, some peaks in the FDD results could not be identified. Presumably, this is caused by the lack of information on the building such as unidentified behavior of the building as a result of lack of excessive installment of sensors on the building or inappropriate modeling of the building.

In the FE modeling phase, several difficulties were observed; one example is related to the complexity of the monitored structure. The building itself is a huge structure with a large number of details. Moreover, there is an unusual structure around the building,

namely, a huge, unsymmetrical shopping mall with many discontinuities. Naturally, several simplifications were made in the FE modeling phase, as the goal of this research was not to obtain a perfect FEM. Some distractions in the way of finding exact values may be created as a result of these simplifications. Nevertheless, as all models will obviously be based on assumptions and simplifications, it cannot be expected to achieve an exact model. Therefore, it can safely be argued that, the model created in this study performed well compared to system identification results of the real building. In general, efforts spent on system identification, and finite element model updating processes show that there are many uncertainties to be clarified and assumptions to be made for more accurate results. Especially the effect of modeling decisions significantly affects the results of the analyses. Assumptions which are made in finite element modeling phase such as the restraining effect due to the shopping center around the tower or the effect of underground part of the structure may lead to significant changes in the results. Moreover, modeling techniques used such as using frame elements or shell elements for modeling the shear walls or the rate of meshing, have a direct effect on the dynamic character of the structure.

The FEM updating process can be considered as very complex for such a huge structure. As there are many uncertainties in the modeling phase, an approximate model leads to an approximate updating process. Material property of the concrete used in the building, namely the modulus of elasticity of concrete, is a simple way to represent the stiffness uncertainty of the model in general. The uncertainties on the boundaries of the structure are tried to be modeled with a stick element which can contribute to stiffness of the first five floors as representing the shopping mall around. The uncertainties on the boundaries of the structure, local stiffness differences of elements in the model and the mass representation in the model are some of the main points that can be improved by means of FEM updating in future studies.

In the seismic demand calculations, the drift ratio results show that time history analyses based on updated and non-updated models lead to significantly different results. For instance, in the case of 2% damping ratio, interstory drift ratio obtained from Kobe (2) record is 0.30% for non-updated case, whereas it becomes 0.56% with finite element model updating. Furthermore, in the case of 5% damping ratio, interstory drift ratio

obtained from Northridge (1) record is 0.15%, while it becomes 0.22% with finite element model updating. In addition, the average drift ratios of all time history analysis results for the 2% damping ratio are 0.26% and 0.22% for non-updated and updated models, respectively. The same results for the 5% damping ratio are 0.21% and 0.17% for non-updated and updated models, respectively.

A further conclusion is that reliability estimations based on finite element model updating turn out to be different than non-updated estimations. For example, when the limit drift ratio is set equal to 0.2%, the failure probabilities of updated and non-updated models for 2% damping ratio are 0.4582 and 0.5776, respectively. The same results for the 5% damping ratio are 0.3148 and 0.4445 for updated and non-updated models, respectively. As an example is the following: in order to inspect the behavior around the tail region of the density functions, when the limit drift ratio is 0.5%, the failure probabilities of updated and non-updated models for 2% damping ratio are 0.0429 and 0.0938, respectively, whereas the results for the 5% damping ratio are 0.0116 and 0.0357 for updated and non-updated models, respectively. Therefore, the difference between updated and non-updated failure probabilities increases dramatically around the tails of probability density functions.

It should be noted that the current identification procedure is able to update FEM effectively in terms of natural frequency, but the error due to higher modes tends to increase as a result of updating. Therefore; even though the first mode of vibration is dominant on dynamic characteristics of the structure; higher modes, especially in tall buildings like the one studied in this paper, should be considered as well. Nevertheless, current results point out significant difference between seismic demands obtained from updated and non-updated models, which might be critical since seismic demand is underestimated in the non-updated case.

Further studies may involve modifications in the structural parameter identification procedure to obtain more reliable outcomes. Extracting modal parameters in a better fashion lead to more realistic results. Moreover, finite element modeling process may be done it more detail. This is due the importance of modeling phase as there are many

assumptions done here by definition. That will directly affect the outcomes in order to get closer to identified parameters. Furthermore, FEM updating algorithm may be realized in alternative ways in order to optimize the process. FEM updating is a crucial part of identification process in overall. Therefore, in order to get a final FEM which reflects the real structure with minimum error, different FEM updating strategies may be followed. Beside these phases, seismic demand analysis strategies also show a wide variety from selection of ground motions to type of analyses applied. In conclusion, even the current state of the methodology shows that drift ratios, and therefore, the seismic demand is sensitive to changes due to identified parameters; and such changes should essentially be investigated in order to assess structural performance accurately.

# REFERENCES

ACI Committee 318, 2008, "Building Code Requirements for Structural Concrete (ACI 318-08) and Commentary", *American Concrete Institute*, Farmington Hills, MI.

Beck, J.L. and P.C., Jennings, 1980, "Structural Identification Using Linear Models and Earthquake Records", *Earthquake Engineering and Structural Dynamics*, Vol. 8, No. 2, pp. 145-160.

Boroschek, R.L. and F.V., Yanez, 2000, "Experimental Verification of Basic Analytical Assumptions Used in the Analysis of Structural Wall Buildings", *Engineering Structures*, Vol. 22, No. 6, pp. 657-669.

Brincker, R., L., Zhang and P., Andersen, 2001, "Modal Identification of Output-Only Systems Using Frequency Domain Decomposition", *Smart Materials and Structures*, No. 12, pp. 441-445

Brownjohn, J.M.W., T.C., Pan and X.Y., Deng, 2000, "Correlating Dynamic Characteristics from Field Measurements and Numerical Analysis of a High-Rise Building", *Earthquake Engineering and Structural Dynamic*s, No. 29, pp. 523-543.

Brownjohn, J.M.W., 2003, "Ambient Vibration Studies for System Identification of Tall Buildings", *Earthquake Engineering and Structural Dynamics*, No. 32, pp. 71–95.

BS EN 1992-1-1 2005, "Eurocode 2: Design of Concrete Structures", *British Standard Institution*, London.

Celebi, M. and E., Safak, 1991, "Seismic Response of Transamerica", *Journal of Structural Engineering*, Vol. 117, No. 8, pp. 2389-2425.

Celebi, M. and E., Safak, 1992, “Seismic Response of Pacific Park Plaza”, *Journal of Structural Engineering*, Vol. 118, No. 6, pp. 1547-1589.

Celebi, M., A., Sanli, M., Sinclair, S., Gallant and D., Radulescu, 2004, “Real-Time Seismic Monitoring Needs Of A Building Owner and the Solution: A Cooperative Effort”, *Earthquake Spectra*, Vol. 20, No. 2, pp. 333-346.

Erdik, M., M., Demircioglu, K., Sesetyan, E., Durukal and B., Siyahi, 2004, “Earthquake Hazard in Marmara Region, Turkey”, *Soil Dynamics and Earthquake Engineering*, No. 24, pp. 605–631.

Ewins, D.J., 2000, “Modal Testing: Theory, Practice and Application”, *Research Studies Press, Ltd.*, Baldock, Hertfordshire, England

Ghanem, R., and M., Shinozuka, 1995, “Structural System Identification”, *Journal of Engineering Mechanics*, Vol. 121, No. 2, pp. 255-273.

Guéguen, P., C., Michel and M., Causse, 2012, “Seismic vulnerability assessment to slight damage based on experimental modal parameters”, *Earthquake Engineering and Structural Dynamic*s, No. 41, pp. 81–98.

Guler, K., E., Yuksel and A. Kocak, 2008, “Estimation of the Fundamental Vibration Period of Existing RC Buildings in Turkey Utilizing Ambient Vibration Records”, *Journal of Earthquake Engineering*, No. 12, pp. 1-11.

Hartmann, D., K., Smarsly and K. H., Law, 2011, "Integration Of Structural Health And Condition Monitoring Into The Life-Cycle Management Of Wind Turbines", *Proceedings of the 4th Workshop on Civil Structural Health Monitoring (CSHM-4)*, November 6, Berlin, Germany.

Jaishi, B., W., Ren, 2005, “Structural Finite Element Model Updating Using Ambient Vibration Test Results”, *Journal of Structural Engineering*, Vol. 131, No. 4, pp. 617-628

Jayaram, N., N., Shome and M., Rahnama, 2012, “Development Of Earthquake Damage Functions For Tall Buildings”, *Earthquake Engineering and Structural Dynamic*s, No. 41, pp. 1495–1514.

Kijewski-Correa, T., A., Kareem and M., Kochly, 2006, “Experimental Verification and Full-Scale Deployment of Global Positioning Systems to Monitor the Dynamic Response of Tall Buildings”, *Journal of Structural Engineering*, Vol. 132, No. 8, pp. 1242-1253.

Kijewski-Correa, T. and J.D., Pirnia, 2007, “Dynamic Behavior of Tall Buildings under Wind: Insights from Full-Scale Monitoring”, *Structural Design of Tall and Special Buildings*, No. 16, pp. 471–486.

Kohler, M.D., P.M., Davis and E., Safak, 2005, “Earthquake and Ambient Vibration Monitoring of the Steel-Frame UCLA Factor Building”, *Earthquake Spectra*, Vol. 21, No. 3, pp. 715-736.

Li, Q.S., J. Q., Fang, A. P., Jeary, C. K., Wong and D. K., Liu, 2000, “Evaluation Of Wind Effects on a Supertall Building Based On Full-Scale Measurements”, *Earthquake Engineering and Structural Dynamic*s, No. 29, pp. 1845 – 1862.

Li, Q.S., Y. Q., Xiao, C. K., Wong and A. P., Jeary, 2003, “Field Measurements Of Wind Effects On The Tallest Building In Hong Kong”, *The Structural Design of Tall and Special Buildings*, No. 12, pp. 67–82

Li, Q.S., J.Y., Fu, Y.Q., Xiao, Z.N., Li, Z.H., Ni, Z.N., Xie and M., Gu, 2006, “Wind Tunnel and Full-Scale Study of Wind Effects on China’s Tallest Building”, *Engineering Structures*, No. 28, pp. 1745–1758.

Li, Y. and S.T., Mau, 1997, “Learning from Recorded Earthquake Motion of Buildings”, *Journal of Structural Engineering*, Vol.123, No. I, pp. 62-69.

Liel A. B., C. B., Haselton, G. G., Deierlein and J.W., Baker, 2009, "Incorporating Modeling Uncertainties The Assessment Of Seismic Collapse Risk Of Buildings", *Structural Safety*, Vol. 31, pp. 197-211.

Lus, H., R., Betti and R.W., Longman, 1999, "Identification of Linear Structural Systems Using Earthquake Induced Vibration Data", *Earthquake Engineering and Structural Dynamics*, No. 28, pp. 1449-1467.

Matlab, 2012, "The Language of Technical Computing", *The MathWorks*, Inc.

Oliveira, C.S. and M., Navarro, 2010, "Fundamental periods of vibration of RC buildings in Portugal from in-situ experimental and numerical techniques", *Bulletin of Earthquake Engineering*, Vol. 8, No. 3, pp. 609-642.

PEER Strong Motion Database, 2005, "The Pacific Earthquake Engineering Research" Center and the University of California.

Republic of Turkey Prime Ministry Disaster and Emergency Management Presidency, 2013, http://www.afad.gov.tr/TR/IcerikDetay.aspx?ID=192, accessed at April, 2013.

Safak, E., 1991, "Identification of Linear Structures Using Discrete-Time Filters", *Journal of Structural Engineering*, Vol. 117, No. 10, pp. 3064-3085.

SAP 2000, "Static and Dynamic Analysis of Structures Ultimate 15.1.0" Computers and Structures, Inc. 1995 University Ave. Berkeley, CA 94704.

Satake, N., K., Suda, T., Arakawa, A., Sasaki and Y., Tamura, 2003, "Damping Evaluation Using Full-Scale Data of Buildings in Japan", *Journal of Structural Engineering*, Vol. 129, No. 4, pp. 470-477.

Skolnik, D.A. and J.W., Wallace, 2010, "Critical Assessment of Interstory Drift Measurements", *Journal of Structural Engineering*, Vol. 136, No. 12, pp. 1574-1584.

Skolnik, D., Y., Lei, E., Yu and J.W. Wallace, 2006, "Identification, Model Updating, and Response Prediction of an Instrumented 15-Story Steel-Frame Building", *Earthquake Spectra*, Vol. 22, No. 3, pp. 781–802.

Smith, R., R., Merello and M., Willford, 2010, "Intrinsic and Supplementary Damping in Tall Buildings", *Structures and Buildings*, No. 163, pp. 111-118.

Soyoz, S. and M.Q., Feng, 2009, "Long-term Monitoring and Identification of Bridge Structural Parameters", *Computer-Aided Civil and Infrastructure Engineering*, Vol. 24, No. 2, pp. 82-92.

Soyoz, S., M.Q., Feng and M., Shinozuka, 2010, "Structural Reliability Estimation with Vibration-based Identified Parameters", *Journal of Engineering Mechanics*, Vol. 136, No. 1, pp. 100-106.

Soyoz, S., E., Taciroglu, K., Orakcal, R., Nigbor, D., Skolnik, H., Lus and E., Safak, 2012, "Ambient and Forced Vibration Testing of a Reinforced Concrete Building Before and After its Seismic Retrofitting", Journal of Structural Engineering, 10.1061/(ASCE)ST.1943-541X.0000568.

Tall Buildings Initiative, 2010, "Guidelines for Performance-Based Seismic Design of Tall Buildings", Report No. 2010/05, *The Pacific Earthquake Engineering Research Center (PEER).*

Tantala, M.W., G., Deodatis, 2002, "Development of Seismic Fragility Curves For Tall Buildings", *15th ASCE Engineering Mechanics Conference*, June 2-5, Columbia University, New York, NY

Turkish Standards Institute, 2007, "Turkish Earthquake Code", Ankara.

Turkish Standards Institute, “TS-500 Building Code Requirements for Structural Concrete”, Ankara.

Wallace, J.W., 2007, “Modeling Issues for Tall Reinforced Concrete Core Wall Buildings”, *The Structural Design of Tall and Special Buildings*, No. 16, pp. 615–632.

Yuen, K.V. and S.C., Kuok, 2010, “Ambient Interference in Long-Term Monitoring of Buildings”, *Engineering Structures*, Vol. 32, No. 8, pp. 2379-2386.

Yun, C.B., and M., Shinozuka, 1980, “Identification of non-linear structural dynamical systems”, *Journal of Structural Mechanics*, Vol. 8, No.2, pp. 187-203.